Effects of Prior Aging at 316 °C in Argon on Inelastic Deformation Behavior of PMR-15 Polymer at 316 °C : Experiment and Modeling

THESIS

Özgür Özmen, First Lieutenant, TUAF

AFIT/GSS/ENY/09-M06

DEPARTMENT OF THE AIR FORCE
AIR UNIVERSITY

AIR FORCE INSTITUTE OF TECHNOLOGY

Wright-Patterson Air Force Base, Ohio

The views expressed in this work are those of author and do not reflect the official policy or position of the United States Air Force, Department of Defense, or the United States Government.

AFIT/GSS/ENY/09-M06

Effects of Prior Aging at 316 °C in Argon on Inelastic Deformation Behavior of PMR-15 Polymer at 316 °C : Experiment and Modeling

THESIS

Presented to the Faculty

Department of Aeronautics and Astronautics

Graduate School of Engineering and Management

Air Force Institute of Technology

Air University

Air Education and Training Command

In Partial Fulfillment of the Requirements for the

Degree of Degree of Master of Science in Space Systems

Özgür Özmen, B.S.E.E.

First Lieutenant, TUAF

March 2009

AFIT/GSS/ENY/09-M06

Effects of Prior Aging at 316 °C in Argon on Inelastic Deformation Behavior of PMR-15 Polymer at 316 °C : Experiment and Modeling

Özgür Özmen, B.S.E.E.
First Lieutenant, TUAF

Approved:

/signed/	10 Mar 2009
Dr. Marina B. Ruggles-Wrenn (Chairman)	date
/signed/	10 Mar 2009
Dr. Richard B. Hall (Member)	date
/signed/	10 Mar 2009
Dr. Greg A. Schoeppner (Member)	date

Abstract

The inelastic deformation behavior of PMR-15 neat resin, a high-temperature polymer, was investigated at 316 °C. The experimental program was designed to explore the influence of strain rate on tensile loading, unloading, and strain recovery behaviors. In addition, the effect of the prior strain rate on the relaxation response of the material, as well as on the creep behavior following strain controlled loading were examined. The material exhibits positive, nonlinear strain rate sensitivity in monotonic loading. Early failures occur in the inelastic range. Nonlinear, "curved" stress-strain behavior during unloading is observed at all strain rates. The recovery of strain at zero stress is strongly affected by prior strain rate. The prior strain rate also has a profound influence on relaxation behavior. Likewise, creep response is significantly influenced by prior strain rate.

The experimental results suggest that the inelastic behavior of the PMR-15 solid polymer at 316 °C can be represented using a unified constitutive model with an overstress dependence of the inelastic rate of deformation. The experimental data were modeled with the Viscoplasticity Based on Overstress (VBO) theory. Additionally the effects of prior aging at 316 °C in argon on the time (rate)-dependent behavior of the PMR-15 polymer were evaluated in a series of strain controlled experiments. Based on experimental results, it was stated that the specimens, which are subjected to prior aging in argon for more than 50 h, generally exhibit only quasi-linear behavior until failure.

Acknowledgements

First and foremost, I owe a large debt of appreciation to Dr. Marina Ruggles-Wrenn for her exceptional guidance and support during this effort. I would like to thank Dr. Richard Hall, and Dr. Greg Schoeppner for serving as members of my advisory committee. I would also like to thank the AFIT Materials Testing Laboratory staff Jay Anderson, Barry Page and Chris Zickefoose for their assistance keeping the experimental equipment operational and John Hixenbaugh for his assistance with the argon gas and aging. Following that, I would like to thank Amber McClung for her assistance during experimental setup process and also for her great help through the modeling portion of this study. Finally, I would like to thank First Lt. Tufan Yeleser, First Lt. Muzaffer Ozer and First Lt. Gokhan Altin for their friendship and assistance throughout this effort. And of course, I would like to express my gratitude to my wife for supporting me from Turkiye and never letting me feel alone.

Özgür Özmen

Table of Contents

Page

List of Figures

List of Tables

Effects of Prior Aging at 316 °C in Argon on Inelastic Deformation Behavior of PMR-15 Polymer at 316 °C : Experiment and Modeling

I. Introduction

The relentless desire of the aerospace industry to build an aircraft that have a reduced weight while improving the structural durability and integrity increases the drive for the high performance structural materials. The composite materials are the main part of this research and the possible advantages of using composites as compared to traditional metals and alloys include reduced costs due to lower production costs, long-term durability and reduced maintenance requirements; higher strength-to-weight ratios and strength and stiffness; lighter weight and the opportunity to design larger parts; corrosion or weather resistance; low thermal conductivity and coefficient of expansion [1]. Polymer matrix composites (PMC's) meet well with these expectations and are in fact used in many aircraft components today. Polymer matrix composites first played a considerable role in military uses. In the 1970s fighter aircraft such as the F-14, F-15, and F-111 had 2 to 4 percent by weight carbon-epoxy composites [2]. By the 1980's it spreaded to the whole aerospace industry and many low speed aircrafts such as the Boeing 757 and McDonnell Douglas MD-80 series contained components made of epoxy resins reinforced with aramid, carbon, and E-glass fibers [3]. By the 1990s, the amount of polymer matrix composites used in fighter vehicles grew to 15 to 30 percent in aircraft such as the A-6, AV-8, F-18, and F-22 by weight [2].

The use of lightweight polymer composites has increased the structural capability of aircraft while reducing weight, resulting in better performance. As an example it decreased fuel consumption in the new Boeing 787 Dreamliner, which was designed with a lightweight composite fuselage and wings [1]. While these composites fit well

into this role, the epoxy resins were limited to operating temperatures below 130 °C [4]. Therefore, the research for some aggressive polymer systems that could stand up to the temperatures beyond that of the epoxy resins has ever existed. The result was an intense investigation of a group of polymers called polyimides which are recognized today as extremely stable and environmentally resistant polymer systems [5]. Polyimides are appealing for their use as matrix resins for high-temperature composite applications due to their high toughness, high tensile strength, high modulus, and resistance to temperature and solvents [5]. The present investigations concentrate on applying lightweight High Temperature Polymer Matrix Composites (HTPMCs) mostly into aircraft engine and structural components. Thermosetting polymers are widely used as matrix materials in fiber-reinforced composites in a broad range of applications, including aerospace, automotive, and oil and gas industries [6,7]. Designing with these materials requires a good understanding of the mechanical behavior (such as shock, impact, loadings, or repeated cyclic stresses) that might cause delamination and degrade performance, either immediately or in the future. Also it is not suitable to predict only the composite's behavior; to analyze the behavior of the composite material, it is critical to evaluate the contribution of the matrix to the overall response of the composite [6].

The efforts at the Air Force Institute of Technology demonstrated that polymers exhibit rate-dependent behavior [4, 8–11]. It was also demonstrated that this rate-dependent response is not represented by linear or nonlinear viscoelasticity; on the other hand the rate-dependent viscoplasticity has been a promising solution to model the mechanical response of these polymers. The Viscoplasticity Based on Overstress (VBO) has been demonstrated to account for some aspects of the deformation behavior of solid polymers [9, 12–19] . Regarding the experimental findings, a specialization of this model for polymers, the Viscoplasticity Based on Overstress for Polymers (VBOP), has been developed [9, 15, 17, 18].

Recent efforts showed that thermal aging has a significant role on the mechanical properties of polymers [9, 20–23] and PMC's [9, 24–26]. Since aerospace components

operate at high temperatures for long periods of time, thermal aging of structural components having polymers appears as a critical problem. So in order to have a more reliable prediction of the material behavior the effects of prior aging must be incorporated into design and analyses procedures, and also a comprehensive model must be established and validated.

There have been many different PMR resins developed but out of several types of polymer resins PMR-15 (Polymerization of Monomeric Reactants-15) is selected and investigated due to its superior high temperature properties and ease of processing [6, 7, 9, 22]. The PMR-15 is designed for use at temperatures near its glass transition temperature, and it is extensively used as a matrix material in high temperature structural composites for aerospace applications [6, 9]. Composites utilizing PMR-15 as matrix material are capable of service temperatures up to 300 °C [6, 27]. For composites incorporated mainly at high temperatures, it is essential to develop a predictive model for the overall behavior of the composite itself. The objective of this research is to evaluate the effects of prior thermal aging at 316 °C in inert gas environment on inelastic deformation behavior of PMR-15 high-temperature polymer at 316 °C and incorporate these effects into the comprehensive model.

The subsequent sections will give enhanced information about the procedure and the results of this research. To begin with a background of composite materials which is mostly focusing on High Temperature Polymer Matrix Composites (HTPMCs) and a background of constitutive modeling will be discussed. A broad discussion of the observed mechanical behavior of polymer materials will also be provided in this chapter. Theoretical formulation of Viscoplasticity Based on Overstress will be given in the subsequent chapter. And afterwards a definition of the test material and the experimental setup and procedures that are used for testing will be explained. The presentation of experimental results will be coming next. Finally, recommendations for future efforts and conclusions will be given.

II. Background

This chapter provides a general overview of polymer matrix composites (PMCs) including a description of polymers and their specific use as neat resins in composite materials. Subsequently, the basic concepts of polymer aging will be reviewed. The Problem Statement and Methodology of this effort will be summarized. Finally, a summary of previous efforts involving PMR-15 and the modeling of high-temperature polymer deformations will be given and the objective of this research will be stated.

2.1 Polymer Matrix Composites

Composite materials are usually classified with respect to the characteristics of the matrix material, i.e. polymer matrix composites (PMCs), metal matrix composites (MMCs), ceramic matrix composites (CMCs). A composite, by definition, is a "material system consisting of two or more phases on a macroscopic scale, whose mechanical performance and properties are designed to be superior to those of the constituent materials acting independently" [4, 28]. In the case of polymer matrix composites (PMCs), one phase of the composite is a polymeric material. The term "polymer" actually applies to a large class of natural and synthetic materials with a variety of properties and purposes. Actually, a polymer is a "macromolecule that contains many groups of atoms, called monomeric units" covalently bonded together [29]. Polymers are often classified into three groups based upon their thermomechanical properties. These groups are can be stated as: thermoplastics, elastomers, and thermosets [4].

Thermoplastics, commonly known as plastics, become fluid when heated and can be easily processed using techniques such as injection molding and extrusion [29, 30]. Further, thermoplastics can also be divided into two classifications: amorphous and crystalline. While thermoplastics that are capable of some crystallization upon cooling are called crystalline polymers and characterized by their melting temperature, Tm; those that are incapable of crystallization are called amorphous polymers and characterized by their glass transition temperature, T_g, at which they transform sud-

denly from a "glassy" hardstate to a "rubbery" soft state [4]. At the temperatures lower than their T_g, amorphous polymers are in a "frozen'" position, but once the temperature goes beyond the T_g limit they can move freely [30].

Elastomers, commonly known as rubbery polymers, are cross-linked polymers that can be easily deformed many times beyond their original length and can also recover rapidly their original dimensions upon release of the applied force [4]. Rubber and neoprene can be stated as the best known examples of the elastomers. Thermoset polymers are the most common types of matrix systems [28]. The structure of these polymers is subjected to a high degree of cross-linking during their curing process. As a result, thermosets cannot be reshaped after their original formation and decompose thermally at high temperatures [28, 30]. Unsaturated polyesters, epoxies, vinylesters, and polyimides are among the most commonly used types of thermosets [28]. Epoxies generally have better mechanical properties than the other thermoset polymers, whereas polyimides are best known for their abilities to withstand higher temperatures.

In the composites the fibers provides the stiffness and the strength whereas the matrix are used for protection and support for the fibers. Polymers are used as matrices in PMCs and PMCs are generally used for load-bearing structures in aviation and space applications for their many advantages including: light weight, high specific strength and stiffness and increased flexibility of design. Depending on their reinforcement phase distributed throughout the matrix, PMCs can be classified in a variety of forms. Continuous-fiber reinforced, particulate-reinforced, and even nanoparticle filled materials may be classified as PMCs [2, 4]. While in high-performance structural applications PMCs typically consist of micron-diameter fibers bound in a polymer resin material, in lower performance composites it is possible for the matrix to be the main load bearing constituent for the material [4].

2.2 Polymer Aging

All polymers go through some amount of degradation when exposed to temperatures at which their covalent bonds start to break down. Chain scission and additional cross-linking occur, both changing material's mechanical properties and degrading the polymer chain. Polymer degradation takes place quickly when it is subjected to temperatures well beyond its glass transition temperature [9, 22]. At lower temperatures, degradation occurs at a much slower rate; consequently the mechanical properties and material behaviors change slowly over time as well [9, 20, 21]. And this can be often observed as a material gets brittle and stiff after extended exposure to higher temperatures.

"Ageing" is a term used in many branches of polymer science and engineering when the properties of the polymer change over a period of time. The changes may be observed in engineering properties such as strength and toughness; in physical characteristics such as density; or in chemical characteristics such as reactivity towards aggressive chemicals. The origins of the changes may be independent of the surrounding environment and may be chemical, as in the case of the progressive cure of a thermosetting material, or physical, as in the case of a rapidly cooled polymer undergoing volumetric relaxation. In other cases the changes may be the result of interaction with the environment, such as when oxidation leads to chain scission. Sometimes a number of age-related phenomena operate simultaneously and/or interactively [31]. Krempl [32,33] defined prior aging as the diffusion process with chemical reactions which occur in the absence of deformation and defined strain aging as the diffusion process with chemical reactions which are initiated by deformation.

For the purpose of this study, the following definitions are assumed:

- prior aging: mechanical property or material behavior changes caused by exposure to elevated temperature prior to deformation
- strain aging: mechanical property or material behavior changes caused by deformation [9, 32].

The current research focuses on the effects of prior aging on the mechanical properties and material behavior of PMR-15. Recent efforts [20,21] revealed that the effects of the strain aging were negligible under the condition that the duration of the deformation or loading was less than 50 hours. Since the current experiments last less than 50 hours, this assumption can be considered as reasonable.

2.3 Problem Statement

High Temperature Polymer Matrix Composites (HTPMCs) in aerospace applications, such as turbine engines and high-speed aircraft skin, must operate in extreme hygro-thermal environments. Failure of composites in these aggressive environments has a direct impact on operational cost and fleet readiness. To assure long-term durability and structural integrity of HTPMC components reliable, experimentally-based life-prediction methods must be developed. Through understanding of aging and deformation mechanisms and their synergistic effects on mechanical behavior HTPMC constituent materials is critical to development of predictive models and methodologies. Key technical issues are the degrading effects that long term exposure to elevated temperature, moisture and oxidizing environment as well as cyclic and creep loading can have on the dimensional stability, strength and stiffness of HTPMC aerospace structures.

2.4 Thesis Objective

The objective of this research is to evaluate the effects of prior thermal aging at 316 °C in inert gas environment on inelastic deformation behavior of PMR-15 high-temperature polymer at 316 °C. Monotonic constant strain rate loading/unloading tests to failure, constant strain rate loading/unloading tests with intermittent periods of relaxation, strain rate jump tests and creep tests will be performed at 316 °C on the unaged material. Then the test program will be repeated for specimens aged at 316 °C in argon for various durations. Results of this research will be used to establish parameters of Viscoplasticity Based on Over Stress (VBO) constitutive model at 316

°C. For same loading histories predictions of the stress-strain response will be obtained using VBO. Model predictions will be compared to experimental results.

2.5 Methodology

The key technical issues summarized in the problem statement were evaluated by the following steps:

1. Document the room temperature elastic modulus of the neat resin to capture the specimen to specimen variability in the elastic modulus
2. Age the samples for various duration in argon environment at elevated temperature
3. Explore the effect of prior strain rate on monotonic stress-strain behavior in monotonic tests at several constant strain rates.
4. Conduct experimental investigations to verify whether the PMR-15 exhibits the strain rate history effect.
5. Explore the effect of prior strain rate on creep behavior in creep tests preceded by uninterrupted loading to a target strain where strain rate will be changing from test to test.
6. Study the relaxation behavior in monotonic test with intermittent periods of relaxation of fixed duration.
7. Demonstrate the ability of the VBOP to qualitatively model PMR-15 behavior using data from current work.
8. Clarify the effects of prior aging on the deformation behavior of PMR-15 neat resin.
9. Demonstrate the VBOP with prior aging.

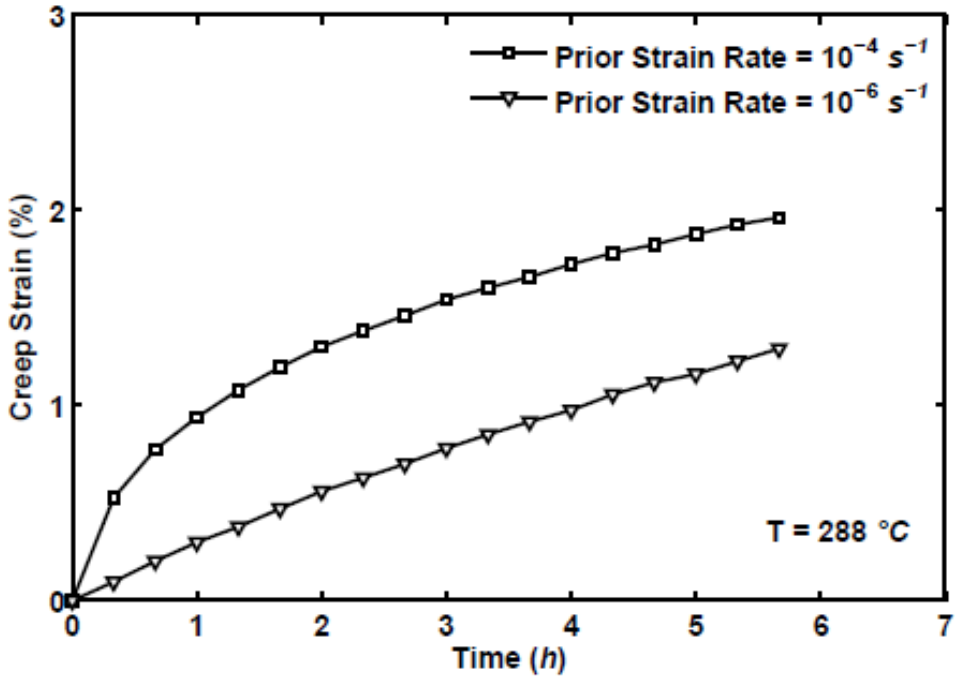

Figure 2.1: Creep strain vs time at 21 MPa and 288 °C. Effect of prior strain rate on creep is apparent. Creep strain increases nonlinearly with prior strain rate.

2.6 Previous Research: Experimental Investigations

2.6.1 PMR-15 - Mechanical Behavior at Room and Elevated Temperatures. The time dependent behavior of PMR-15 was studied by Westberry [10] at room temperature and at 288 °C. Westberry conducted tests using different stress rates at 23 °C and 288 °C. Westberry reported that at 288 °C, PMR-15 polymer exhibits rate dependent behavior in both creep and recovery tests. Falcone and Ruggles-Wrenn [8] explored the effect of prior stress rate on creep behavior of PMR-15 neat resin at 288 °C. These results also showed that the creep behavior of the material is dependent upon the prior stress rate. They also conducted monotonic loading/unloading tests at various constant stress rates and reported that the material response was also dependent upon the rate of loading/unloading.

McClung and M.B. Ruggles-Wrenn [6] investigated the inelastic deformation behavior of PMR-15 neat resin at 288 °C. These experimental results revealed the

rate dependence of the inelastic deformation. Creep response of PMR-15 at 288 °C reported in Reference [6] is reproduced in Figure 2.1. They reported [6] the following conclusions;

1. PMR-15 polymer exhibits positive nonlinear strain rate sensitivity during monotonic loading and unloading.
2. There is no strain rate history effect.
3. The recovery of strain at zero stress is strongly influenced by prior strain rate. The recovery rate increases with prior strain rate
4. The creep behavior is also profoundly affected by the prior strain rate. The creep rate at the same stress level increases with prior strain rate.
5. The relaxation behavior is influenced by prior loading rate. Once the inelastic flow is fully established, the stress change during relaxation depends only on time and prior strain rate and is independent of the stress and strain at the beginning of relaxation.

2.6.2 Prior Aging - Effects on Mechanical Behavior. Krempl [33, 34] stated that the effects of aging should be separated from other factors in order to obtain valid conclusions. He pointed out that tests must be repeated with specimens that have seen different durations of prior aging in order to examine the effects of exposure and described a procedure to test for prior aging effects, in which the material is exposed to step changes in strain rate.

Ruggles and Krempl [35] investigated the effects of prior aging on AISI Type 304 stainless steel and found that prior aging did not have significant influence on the material behavior. On the other hand they observed that the material response was more influenced by strain aging.

Ruggles-Wrenn and Broeckert [21] examined the effects of prior aging in air and in argon at 288 °C on PMR-15 neat resin. They studied the weight loss, changes in dynamic modulus, and the growth of oxidative layer with prior aging time. They

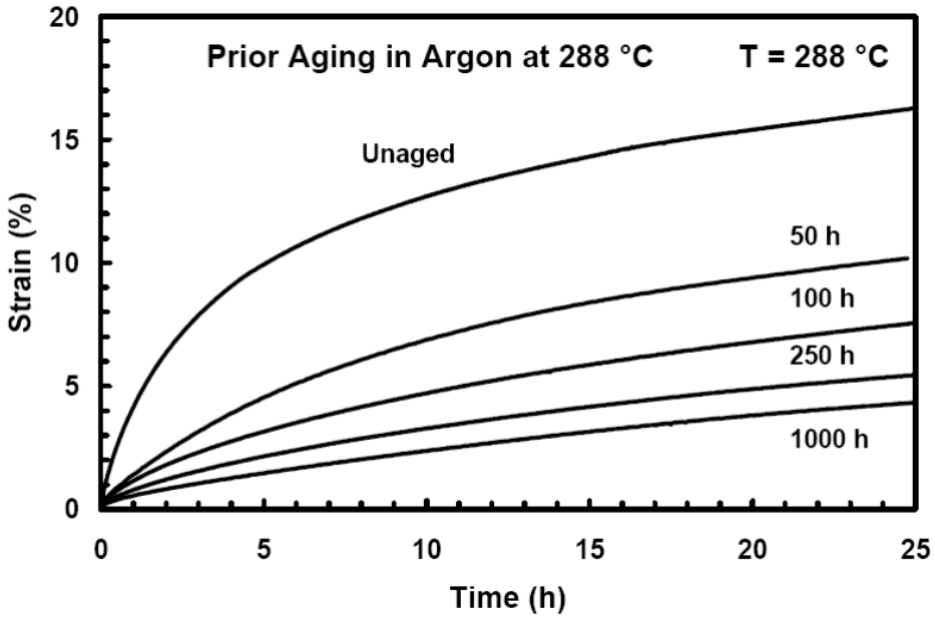

Figure 2.2: Creep strain vs time at 20 MPa and 288°C for the PMR-15 specimens aged at 288°C in argon. Effect of prior aging time on creep strain is apparent.

stated that the material develops an oxidative layer when aged in air, but not in argon. They also explored the effects of prior aging on the elastic modulus and the creep behavior. In spite of the difference in oxidative layer growth, it was observed that specimens aged in air and those aged in argon exhibited similar changes in elastic modulus and creep behavior. They stated that the elastic modulus increased with prior aging time and also reported that accumulated creep strain decreased with an increase in prior aging time. Creep response of PMR-15 at 288 °C reported in Reference [21] is reproduced in Figure 2.2.

McClung investigated the effects of prior aging on deformation behavior of the PMR-15 at 288 °C. McClung demonstrated [9] that the prior thermal aging in argon significantly influences the mechanical behavior of the PMR-15 neat resin and reported [9] the following results;

1. The elastic modulus and the tangent modulus of the material increases with increasing aging time.

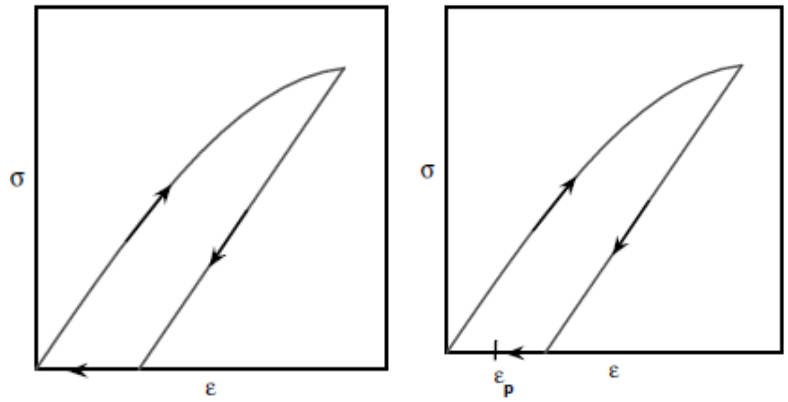

(a) Viscoelasticity (b) Viscoplasticity

Figure 2.3: Viscoelastic and Viscoplastic Stress-Strain Behavior.

2. The flow stress increases with increasing aging time.

3. Departure from quasi-linear behavior is delayed with increasing aging time.

2.7 Previous Research: Constitutive Modeling

2.7.1 Viscoplasticity Based on Overstress. The concept of modeling material response can be explained with the viscoplastic behavior. This type of behavior can be observed in the laboratory with PMR-15. Figure 2.3 shows a graphical comparison of (a) viscoelastic behavior and (b) viscoplastic behavior.

Viscoelastic behavior is characterized by nonzero strain upon immediately after unloading to zero stress. The strain, however, goes back to zero with time. Viscoplastic behavior, sometimes referred as rate dependent plasticity, is also characterized by nonzero strain immediately after unloading to zero stress. But in the viscoplastic case the strain does not go back to zero even if given infinite time to recover, a permanent strain is inevitable. There are many viscoplastic models based on varying microstructural or phenomenological bases. The focus of the current discussion is Viscoplasticity Based on Overstress (VBO).

Krempl and his co-workers have developed the viscoplasticity based on overstress (VBO) over the years. It is a unified viscoplastic constitutive model, meaning that

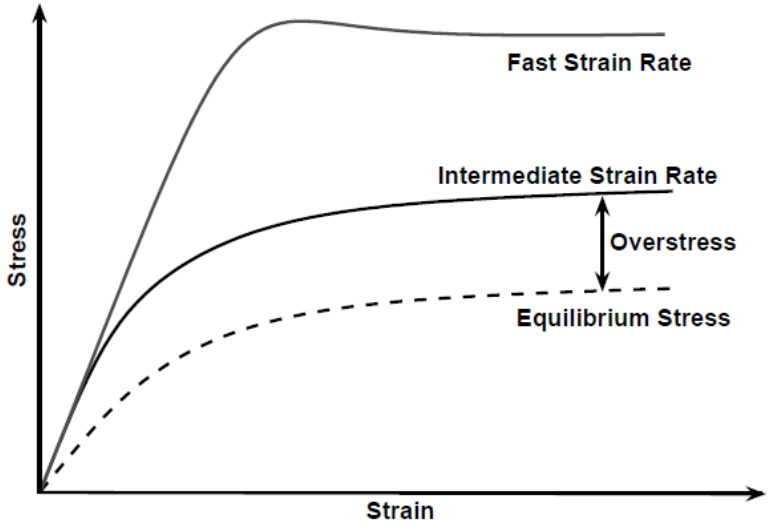

Figure 2.4: Standard Linear Solid Stress-Strain Behavior. The Equilibrium Stress and the Overstress are also Shown .

creep strain and plastic strain are not represented by separate terms in the constitutive equations [9]. The VBO model includes the overstress concept. Overstress is defined as the difference between the flow stress and the equilibrium stress. The flow stress is the applied stress in the region of fully developed plastic flow. The equilibrium stress is a theoretical stress-strain curve conducted at an infinitesimally small strain rate. It can be defined as the stress sustained at rest and sometimes even referred as rest or back stress [36]. Figure 2.4 shows a schematic depicting the flow stress and the equilibrium stress as functions of strain as well as the overstress.

The overstress concept in viscoplasticity has been introduced in dynamic plasticity by Malvern and for static viscoplasticity by Perzyna [37]. The usefulness of the overstress concept in explaining unusual and even paradoxical experimental results has been demonstrated by Krempl with state variable theories [37]. The viscoplastic models make the inelastic strain rate a function of the overstress. For the uniaxial state of stress with σ and ϵ denoting the engineering stress and infinitesimal strain respectively, the model is given by the two coupled nonlinear differential constitutive equations [38]

$$\dot{\epsilon} = \dot{\epsilon}^{el} + \dot{\epsilon}^{in} = \frac{\dot{\sigma}}{E} + \frac{\sigma - g}{Ek\,[\sigma - g]} \tag{2.1}$$

$$\dot{g} = \Psi[\,]\dot{\epsilon} - \frac{g - f[\,]}{b[\,]}|\dot{\epsilon}^{in}| \tag{2.2}$$

where square brackets denote "function of" E is the elastic modulus, k is the viscosity function, g equilibrium stress and Ψ, f, b are the arguments which will be determined in the sequel.

In examining the mathematical properties of nonlinear differential constitutive equations it was shown by Cernocky and Krempl that making the inelastic strain rate solely dependent on the overstress gives qualitative solution properties of the differential equations found in corresponding experiments [38]. This approach has been verified for monotonic loading of Type 304 Stainless Steel and of a Ti-alloy by Krempl and by Kujavski and Krempl, respectively [38]. Following the procedures of Cernocky and Krempl the constitutive equations [4] and [20] were transformed to integral relations [38].

The replacement of the engineering alloys with the solid polymers in some load bearing structures increased the need to predict more accurately the behavior of the solid polymers [9]. Bordonaro [12] and Krempl and Bordonaro [13] demonstrated specific features of mechanical behavior of polymers (specifically Nylon-66, PEEK, and PEI) which the standard VBO could not capture. These features include higher relaxation rates, increased strain recovery after unloading to zero stress, curved unloading in stress control, reduced rate-dependence in unloading, and merging of the stress strain curves produced at different strain rates [9]. Khan [14] demonstrated that the standard VBO can successfully capture some, but not all of the essential features of polymer mechanical behavior at room temperature.

Based on the findings of Bordonaro's research, the VBO for Polymers (VBOP) was developed [9]. This version was shown to predict the behaviors of Nylon-66 [15,16],

PC [17, 18], PPO [17], and HDPE [18] better than standard the VBO and it should be noted that [9] the VBOP was used to model the behavior of both amorphous (PC, PPO, and PES) and crystalline (Nylon-66, HDPE, PET) polymers.

2.7.2 Viscoplasticity Based on Overstress for Polymers. The experimental results reported by McClung [9] and previously by Falcone and Ruggles-Wrenn [8] revealed several key features of the deformation behavior of the unaged PMR-15 neat resin at 288 °C:

1. Linear, quasi-elastic behavior observed upon initial loading transitions into the region of inelastic deformation (or flow stress region), which is characterized by a low tangent modulus (slope of the stress-strain curve).
2. The unaged PMR-15 neat resin exhibits significant nonlinear strain rate sensitivity in monotonic loading. The flow stress increases nonlinearly with increase in the loading rate.
3. A unique stress-strain curve is obtained for a given strain rate. There the lack of a strain rate history effect in the response to the strain rate jump test.
4. Recovery of strain is strongly influenced by prior strain rate. The recovery rate increases with prior strain rate.
5. Creep rate at a given stress increases with prior strain rate.

McClung [9] reported that the experimental results strongly suggest the usefulness of the overstress concept in the modeling inelastic deformation of the PMR-15 neat resin at 288 °C. To assess the ability of the VBOP to reproduce the essential qualitative features of the PMR-15 inelastic behavior, McClung [9] carried out several VBOP simulations and reported:

1. The VBOP simulations are consistent with the qualitative features of the inelastic behavior exhibited by the PMR-15 at 288 °C. The initial quasi-linear behavior is reproduced.

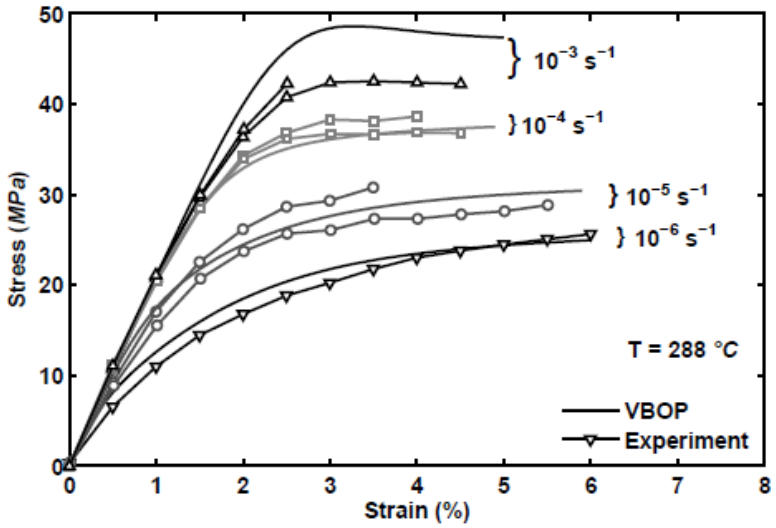

Figure 2.5: A Comparison Between Experimental and Predicted Stress-Strain Curves Obtained for PMR-15 Polymer at Constant Strain Rates of 10^{-6}, 10^{-5}, 10^{-4}, and 10^{-3} s^{-1} at 288 °C. The Model Successfully Represents the Strain Rate Dependence. Reproduced from McClung [9] Fig 7.2

2. The positive, nonlinear rate sensitivity is also evident in monotonic loading.

3. The simulation of the stress-strain behavior in the SRJT clearly demonstrated the absence of the strain rate history effect in the VBOP simulations. The VBOP has no difficulty reproducing "the rapid forgetting" of the prior history that was observed in experiments.

4. The VBOP is capable of reproducing the effect of prior loading rate on relaxation and creep behaviors

McClung [9] also reported that these results suggest the VBOP as a promising candidate constitutive model to represent the deformation behavior of this high-temperature polymer and except for the unloading behavior, the predictions of the material response under both strain-controlled and stress-controlled tests histories were in good agreement with the experimental data.

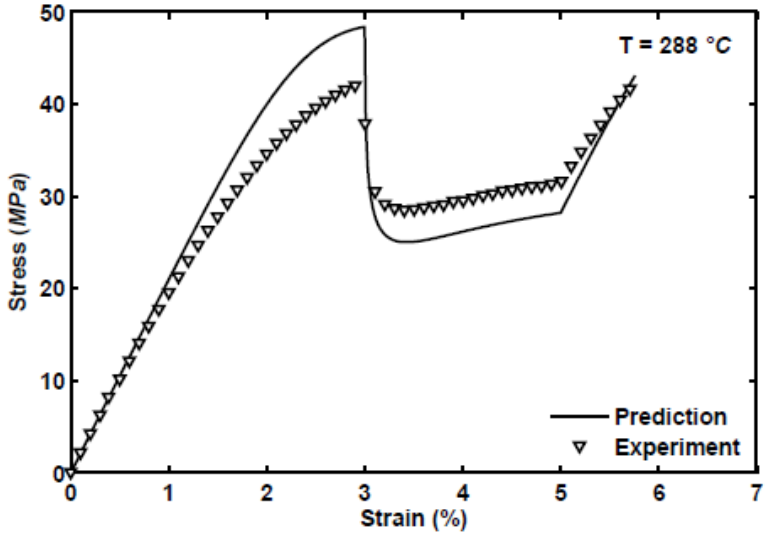

Figure 2.6: A Comparison Between Experimental and Predicted Stress-Strain Curves Obtained for PMR-15 Polymer in the Strain Rate Jump Test at 288 °C. The Model Successfully Represents the Behavior Upon a Change in Strain Rate.Reproduced from McClung [9] Fig 7.4

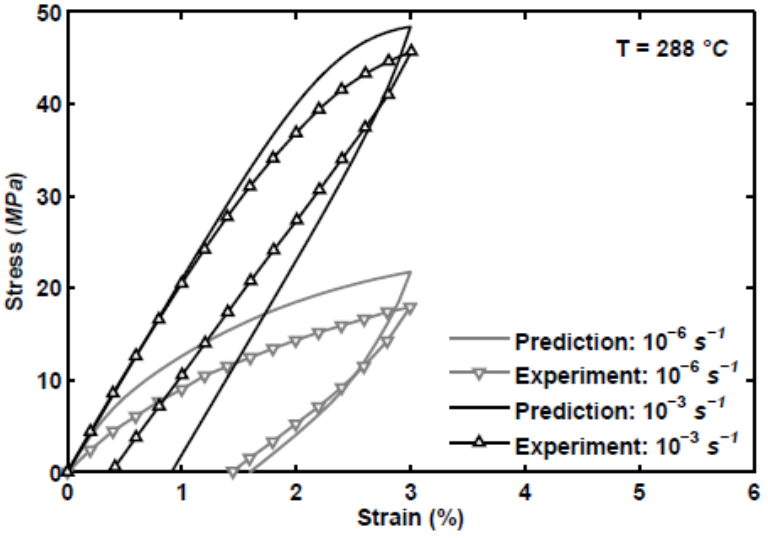

Figure 2.7: A Comparison Between Experimental and Predicted Stress-Strain Curves Obtained for PMR-15 Polymer in Loading and Unloading at Two Constant Strain Rates at 288 °C. The Model Successfully Represents the Strain Rate Dependence on the Unloading. Reproduced from McClung [9] Fig 7.5

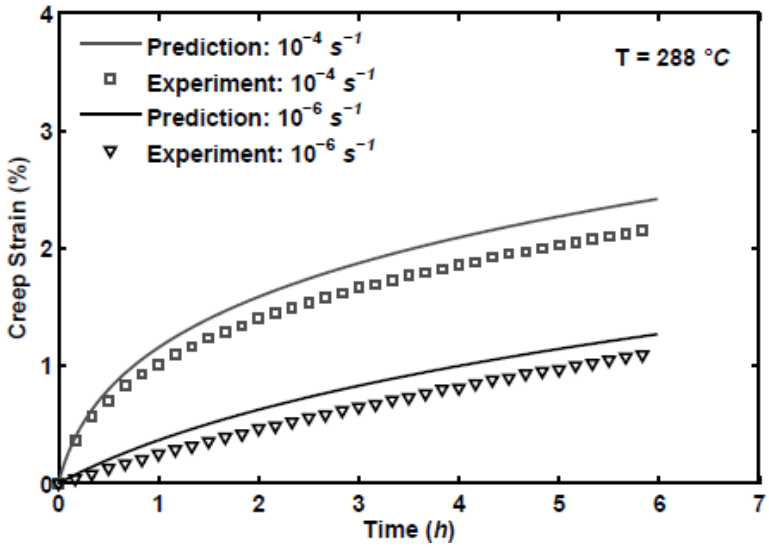

Figure 2.8: Comparison Between the Experimental and Predicted Strain vs Time Curves Obtained for PMR-15 Polymer at 288 °C in Creep at 21 MPa. Prior Loading at Strain Rates of 10^{-6} and 10^{-4} s^{-1}. Reproduced from McClung [9] Fig 7.4

2.7.3 Viscoplasticity Based on Overstress for Polymers with Prior Aging. As was discussed in the previous section, McClung [9] reported four features of material behavior that are influenced by prior aging duration.

1. Increase in initial slope of the stress-strain curve
2. Increase in final slope of the stress-strain curve
3. Increase in flow stress in the region of plastic flow
4. Delayed departure from quasi-linear behavior

Based on these considerations, these features were tied to specific parameters within the VBOP formulation to account for the changes in deformation behavior due to prior aging:

1. Elastic modulus E increases with increasing prior aging time.
2. Tangent modulus E_t increases with increasing prior aging time.
3. Isotropic stress A increases with increasing prior aging time.

4. Shape Parameter C_2 increases with increasing prior aging time.

Then the VBOP parameters were determined for specimens subjected to prior aging of various durations using the developed model characterization procedures and were validated using the experimental results for PMR-15 neat resin subjected to 2000 h prior aging in both strain-controlled tension to failure tests and in creep at 21 MPa. McClung [9] reported that the VBOP predicted accurately the behavior of the material subjected to prior aging for 2000 h.

III. Theoretical Formulation of Viscoplasticity Based on Overstress for Polymers

This chapter focuses on the theory of Viscoplasticity Based on Overstress for Polymers (VBOP). The VBOP is chosen to model the behavior of PMR-15 at 316 °C. The current research also expands the VBOP to include prior aging. A good understanding of the VBOP is needed before the introduction of aging into the model formulation can be discussed. It is important to note that both the VBO and the VBOP are unified viscoplastic constitutive models meaning that inelastic strain is not separated into creep strain and plastic strain

3.1 Basis of Viscoplasticity Based on Overstress - Standard Linear Solid

This section describes the Standard Linear Solid (SLS). It was shown that overstress viscoplastic constitutive law can be traced back to the Standard Linear Solid (SLS) of viscoelasticity [37].The Standard Linear Solid (SLS) is the model upon which the VBO is based. It is called solid since it is capable of maintaining nonzero stress for infinite time in relaxation motions, when the strain rate is zero or the strain is kept constant [37]. The mechanical model of the Standard Linear Solid (SLS) is depicted in Figure 3.1

The constitutive equation of the Standard Linear Solid (SLS) is

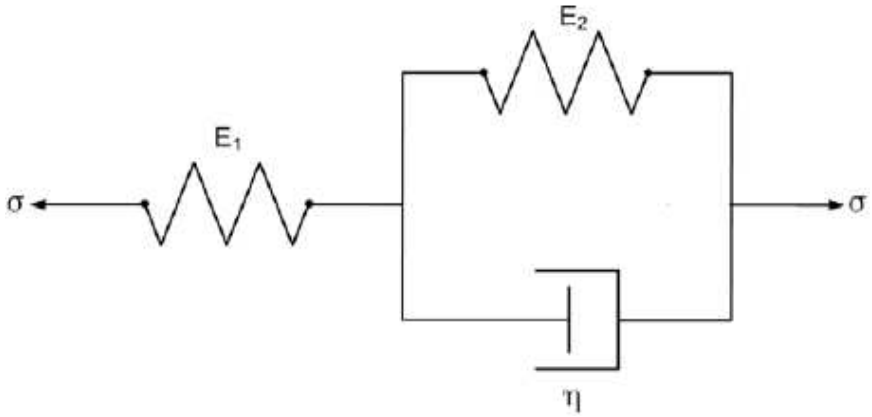

Figure 3.1: Standard Linear Solid (SLS).

$$\dot{\epsilon} + \frac{E_2}{\eta}\epsilon = \frac{\dot{\sigma}}{E_1} + \left(\frac{E_1 + E_2}{E_1}\right)\frac{\sigma}{\epsilon} \tag{3.1}$$

where E_i is the elastic constant of the spring "i" and η is the viscosity constant of the dashpot. The Standard Linear Solid (SLS) is the simplest linear Viscoelastic solid that shows both creep and relaxation [37].

3.2 Viscoplasticity Based on Overstress

The strain rate in the standard linear solid constitutive equation can be divided into elastic, $\dot{\epsilon}^{el}$ and inelastic, $\dot{\epsilon}^{in}$ parts. The constitutive equation can then be rearranged into the following overstress form [9],

$$\dot{\epsilon} = \dot{\epsilon}^{el} + \dot{\epsilon}^{in} = \frac{\dot{\sigma}}{E} + \left[\frac{\sigma}{a\eta} - \frac{E_2}{\eta}\epsilon\right] \tag{3.2}$$

or

$$\dot{\epsilon} = \dot{\epsilon}^{el} + \dot{\epsilon}^{in} = \frac{\dot{\sigma}}{E_1} + \frac{\sigma - aE_2\epsilon}{a\eta} \tag{3.3}$$

where

$$a = \frac{E_1}{E_1 + E_2} \tag{3.4}$$

The term $\sigma - aE_2\epsilon$ is referred to as the overstress and the term $g = aE_2\epsilon$ is called equilibrium stress. The equilibrium stress, identified as the generally path-dependent stress that can be sustained at rest and is a measure of the defect structure and the elasticity of the material.

The material behaves differently depending on loading rate, as illustrated in Figure 2.4. Extremely slow loading corresponds to the equilibrium stress curve which is governed by the two springs in series $(E_1E_2)/(E_1 + E_2)$ [9]. Extremely fast loading provides a linear upper bound to the material behavior and is governed by E_1 [9, 37].

The constitutive equations are made nonlinear by making the spring modulus E_2 a nonlinear function of strain and by making the viscosity η a function of overstress [9,37]. The final step needed to develop the standard VBO is to change the equilibrium stress to have a "proper hysteretic behavior" [9, 37].

The governing equation of the standard VBO is as follows [9, 36]:

$$\dot{\epsilon} = \frac{\dot{\sigma}}{E} + \frac{\sigma - g}{Ek} \tag{3.5}$$

where E is the elastic modulus, g is the equilibrium stress, and k is the viscosity function. The growth law for the equilibrium stress is [9]:

$$\dot{g} = \Psi \frac{\dot{\sigma}}{E} + \frac{\Psi}{E}\left[\frac{\sigma - g}{k} - \frac{g - f}{A}\frac{(\sigma - g)}{k}\right] + \left(1 - \frac{\Psi}{E}\right)\dot{f} \tag{3.6}$$

where A is the isotropic (rate-independent) stress, Ψ is the shape function, and f is the kinematic (rate-dependent) stress. The basic form of the viscosity function [9] is:

$$k = k_1 \left(1 + \frac{|\sigma - g|}{k_2}\right)^{-k_3} \tag{3.7}$$

where k_1, k_2, and k_3 are material constants. This function acts as a repository for modeling rate dependence [31]. The evolution of the isotropic stress is [9]:

$$\dot{A} = A_c[A_f - A]\left|\frac{\sigma - g}{Ek}\right| \tag{3.8}$$

where A_c is a constant that controls how quickly saturation of cyclic hardening or softening is reached and A_f is the saturated value of A [9]. The isotropic stress A establishes the difference between the kinematic stress and the equilibrium stress [36] and is responsible for modeling cyclic hardening or softening [9]. The recommended basic form for the shape function is given as [9]:

$$\Psi = C_1 + (C_2 - C_1)e^{-C_3|\epsilon^{in}|} \tag{3.9}$$

where C_1, C_2, and C_3 are material constants. The shape function governs the shape of the "knee" in the stress-strain diagram. The evolution of the kinematic stress is given by [9]:

$$\dot{f} = E_t \left(\frac{\sigma - g}{Ek} \right) \tag{3.10}$$

where E_t is the slope of the stress-strain curve in the region where the inelastic (plastic) flow is fully established. The kinematic (rate dependent) stress f governs the slope of the stress-strain curve in the plastic flow region (where inelastic flow is fully established) [38]. The kinematic stress was introduced as a repository for modeling the ultimate tangent modulus of the stress strain curve [9].

A yield surface does not exist in this theory, and it cannot reproduce exactly linear elastic regions since the inelastic strain rate, however small, is always present [36]. The absence of exactly elastic regions has the advantage that recovery of the strain at zero stress, creep in the linear portion of the stress-strain diagram can be modeled without difficulty [36].

Several versions of the VBO exist, each sharing the existence of a flow law and three state variables (equilibrium stress g, isotropic stress A, and kinematic stress f) [9]. The VBO for Polymers has added rate-dependence in the equilibrium growth law and reconfigures some of the functions to better fit typical behavior of the investigated polymers at room temperature [9]. For the present research, the VBO for Polymers is chosen since it is formulated for the class of material that is in the scope of interest.

3.3 Viscoplasticity Based on Overstress for Polymers

Ho [15] developed the VBOP to address the needs reported by Bordonaro and Krempl [19], Bordonaro [12], and Krempl and Bordonaro [13] and it was subsequently used to model the behaviors of various polymers [9]. The governing equation of the standard VBO is still valid [9, 36]:

$$\dot{\epsilon} = \frac{\dot{\sigma}}{E} + \frac{\sigma - g}{Ek} \tag{3.11}$$

The growth law for the equilibrium stress is [9]:

$$\dot{g} = \Psi \frac{\dot{\sigma}}{E} + \frac{\Psi}{E}\left[\frac{(\sigma - g)}{k} - \frac{(g - f)}{A}\left|\frac{(\sigma - g)}{k}\right| + (\dot{\sigma} - \dot{g})\right] + \left(1 - \frac{\Psi}{E}\right)\dot{f} \tag{3.12}$$

But for the VBOP the growth of the equilibrium stress is dependent not only on the overstress, but also on the over-stress rate. This additional term $\Psi/E(\dot{\sigma} - \dot{g})$ influences the rate of equilibrium stress and in turn influences the relaxation rate, allowing the model to capture the higher relaxation rates commonly observed in relaxation of polymers [9]. This additional term is optional, depending on the specific material behavior in question. For the PMR-15 at 288 °C it was reported that [9] the term was not appropriate. Regarding that the term is simply not included in this research. For more information refer to [9]. The viscosity function for the VBOP [9] is:

$$k = k_1 \left[1 + \left(1 + \frac{A_0 - A}{A_0 - A_f}\right)\frac{\Gamma}{k_2}\right]^{-k_3} \tag{3.13}$$

where A_0 is the initial value of A, and k_1, k_2, and k_3 are material constants. The addition of a dependence on the isotropic stress allows for the stress-strain curves at different train rates to merge. This merging is "correlated with the strain dependence of the stress relaxation time" [9, 15]. The term Γ stands for the overstress invariant, and it has the form:

$$\Gamma = |\sigma - g| \tag{3.14}$$

The evolution of the isotropic stress [9] retains the form as in the VBO:

$$\dot{A} = A_c[A_f - A] \left| \frac{\sigma - g}{Ek} \right| \tag{3.15}$$

In the case of many solid polymers, this is simplified by setting $A_c = 0$ and making A constant [9] if the material is cyclically neutral. However, this simplification cannot always be made. One such case is Nylon-66 [15, 16], which exhibits cyclic softening. The recommended basic form for the shape function is given as [9]:

$$\Psi = C_1^* + (C_2 - C_1^*)e^{-C_3|\epsilon^{in}|} \tag{3.16}$$

where

$$C_1^* = C_1 \left[1 + C_4 \left(\frac{|g|}{A + |f| + \Gamma^2} \right) \right] \tag{3.17}$$

and C_1 to C_4 are material constants. The shape function governs the shape of the knee in the stress-strain diagram as well as the curvature of the unloading curve but also it reduces the rate-dependence of the unloading curves [9]. This term is also optional depending on the behavior of the particular material in question. For the PMR-15 at 288 °C it was reported [9] that this term was not appropriate because the unloading behavior of the PMR-15 exhibits strong rate dependence. For more information refer to [9].

The evolution of the kinematic stress takes the form [9]:

$$\dot{f} = \left(\frac{|\sigma|}{\Gamma + |g|} \right) E_t \left(\frac{\sigma - g}{Ek} \right) \tag{3.18}$$

The additional term $(|\sigma|/(\Gamma + |g|))$ increases the strain recovery, by slowing the rate at which the equilibrium stress decreases, after unloading to zero stress [9]. This term is also optional depending on the behavior of the particular material of interest [9].

The modifications discussed above were initially introduced to meet the needs for modeling the behavior of Nylon-66 as discussed by Bordonaro [12] and Ho [15] and as stated by McClung [9]. This form has become known as the VBOP and has been successfully utilized to model the behaviors of other solid polymers at room temperature [9]. The VBOP model stands as an appropriate choice of a constitutive model for capturing the behavior of the PMR-15 in the present research.

IV. Material and Test Specimen

This section will discuss in detail the material under investigation. The actual test specimens will be discussed, including processing of the material, specimen geometry and preparation.

4.1 PMR-15 (Polymerization of Monomeric Reactants-15)

This research focuses on PMR-15 solid polymer which is a thermosetting polyimide used as a matrix material for High Temperature Polymer Matrix Composites (HTPMC's). The PMR-15, developed by NASA Lewis Research Laboratory in the 1970's has become the benchmark of high performance aerospace thermoset polymer resins. It is named for the type of reaction used to manufacture the resin, while the 15 alludes to the average molecular weight of 1500 g/mole of the oligomers before the final cure [20]. The PMR-15 polyimide has a glass transition temperature of 347 °C [20] and a long-term use temperature of 288 °C [7]. But Broeckert reported in his study [20] that the unaged PMR-15 neat resin found to have a T_g of 331 °C. He attributed this discrepancy to the differences in material used or to an unconventional sample geometry used in the tests or different heating rates which has been shown to affect T_g measurements [39, 40]. There have been many different PMR resins developed but none have been accepted and utilized as widely as PMR-15. This highly cross-linked polyimide resin was developed specifically for use in high-temperature aerospace structural applications [9].

4.2 Material Processing

The PMR-15 neat resin panels were supplied and post cured by HyComp Inc. (Cleveland,OH). The standard free standing post cure cycle used by the Air Force Research Laboratory is shown in Table 4.1. It is assumed that each of the panels was exposed to this post cure cycle.

Step	Description
Step 1	Heat to 204°C in 2 h and hold for 1 h
Step 2	Heat to 260°C in 1 h and hold of 1 h
Step 3	Heat to 316°C in 2 h and hold of 16 h
Step 4	Cool to room temperature at a rate of 1°C/min

Table 4.1: Standard post cure cycle for PMR-15 neat resin panels

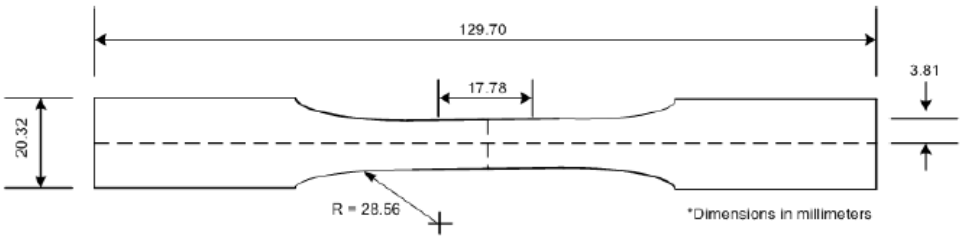

Figure 4.1: The Nominal Test Specimen Geometry

4.3 Specimen Geometry

A reduced gage section or dog bone shaped specimens were used in all test to make sure that if a failure occurs it is the gage section that fails during testing. The panels from which the specimens were cut determined the thicknesses of the specimens. The average thickness of panels used was 3.37 mm while the range of thicknesses encountered in the specimens tested were from 2.69 to 4.32 mm. The average cross sectional area of panels used was 25.57 mm^2 while the range of cross sectional area is encountered in the specimens tested were from 20.41 to 32.87 mm^2. The specimen gage length was 17 mm which fully enables the placement of the extensometer rods with a 12.7 mm gage length. The specimen geometry is shown in Figure 4.1

4.4 Specimen Preparation

The specimens were washed by hand using common hand soap and rinsed in the distilled water to remove any contaminates that might influence the aging process. The gloves were used to handle the samples after this point. The specimens were then dried in a vacuum oven at 105 °C for at least 24 h to ensure that all the moisture was removed. The specimens were held in a desiccator purged continuously with dry air

all the time unless they are tested. The specimens were marked with silver colored permanent marker for distinction and weighed after the specimens marked and dried.

Mechanical testing required the use of a high temperature extensometer therefore each specimen was dimpled before aging and testing. The dimples were placed using a metal punch provided by MTS and a small hammer. The dimple depth was kept as small as possible in size to minimize the possibility of inducing crack propagation from the sites. The effect of the dimples on the UTS was reported by Falcone [4] and was taken into consideration.

Before testing, each specimen was tabbed using a glass fabric/epoxy material to protect the specimens from the aggressive surface of the grips. To tab the specimen, the grip surface area of the specimen was cleaned free of debris and then the tabs were coated with an M-Bond Catalyst. After enough time for the catalyst to dry out, M-Bond 200 adhesive was applied to the tab.

V. Experimental Setup and Testing Procedures

This chapter describes the experimental setup and associated procedures needed to examine the strain rate-dependent behavior of the PMR-15 at 316 °C as well as the effects of prior aging on the inelastic deformation of the material.

5.1 Mechanical Testing Equipment

All mechanical testing was accomplished using a vertically configured Material Test Systems (MTS) servo hydraulic machine equipped with the TestStar II's digital controller for input signal generation and data acquisition. The hydraulic machine employed hydraulic wedge grips which were equipped with an inlet and outlet to allow cooling water to pass through the grips during testing to prevent overheating of the grips. The grip pressure throughout testing of the PMR-15 neat resin was set to 2.76 MPa. The temperature of the specimen gauge section was controlled by an MTS resistance-heated furnace, with an MTS temperature controller. An MTS uniaxial high-temperature extensometer was used for strain measurements. The extensometer includes two 3.5 mm diameter alumina extension rods and has a gauge length of 12.7 mm (0.5 in). The extensometer tips are placed into the dimples on the specimen to avoid slipping of the extensometer during testing. This setup enabled both strain-controlled testing and immediate control mode switching. Figure 5.1 depicts the test setup with the servo hydraulic machine, the furnace, and the extensometer assembly.

5.2 Test Procedures

5.2.1 Room Temperature Elastic Modulus. Before aging and conducting any further testing the initial room-temperature elastic modulus of each specimen was measured in order to capture the sample to sample variability and have a foresight about each specimen. The tests were carried out at room temperature in a laboratory environment. The specimen was loaded to 3 MPa at a rate of approximately 1 MPa/s and unloaded at the same rate to zero stress. The stress level of 3 MPa and the loading rate of 1 MPa/s were chosen to ensure introducing no permanent strain and

Figure 5.1: Test setup with the servo hydraulic machine, the furnace, and the extensometer assembly

having a linear response. The measured elastic modulus of each specimen will be useful for further testing in reducing data scatter with respect to sample to sample variability.

5.2.2 Temperature Calibration. Temperature calibration was performed to ensure to achieve the desired specimen temperature of 316 °C. Two K-type thermocouples were fixed onto a PMR-15 neat resin specimen. The thermocouples were then connected to a two-channel temperature sensor to monitor the specimen temperature in both locations. The oven temperature was elevated to 240 °C at a rate of 2 °C /min subsequently to 260 °C at a rate of 1.5 °C /min and finally to 277 °C at a rate of 1 °C /min and manually increased thereafter. After reaching the target temperature, the oven was allowed to dwell for 2.5 h to ensure that the specimen temperature had thermally equilibrated. During this period, the temperature readings between the left and right thermocouples were within 5 °C of the desired temperature. All tests were carried out at 316 °C in laboratory air environment. In all tests, the specimen was heated to target temperature at a rate of 2 °C/min, and kept resting for an additional 45 min prior to testing.

5.2.3 Monotonic Tensile Test at Constant Strain Rate. Monotonic Tensile Tests at Constant Strain Rates are used to form a baseline for the strain rate dependency of the material. Tensile tests were conducted with the specimens from each aging group including the unaged ones at the strain rates 10^{-6} , 10^{-5} , 10^{-4} and 10^{-3} s^{-1} . The aim of the monotonic testing at multiple constant strain rates is to determine whether and how the flow stress, elastic modulus and tangent elastic modulus change with the strain rate. An example of the effect of the strain rate on the stress-strain behavior of PMR-15 at 288 °C is presented in 5.2 reproduced from McClung and Ruggles-Wrenn [6]

5.2.4 Loading Followed by Unloading at Constant Strain Rate. Loading Followed by Unloading tests were conducted at the strain rates of 10^{-6} , 10^{-5} and 10^{-3} s^{-1} . The specimens were loaded to a fixed strain of 3% and unloaded to zero stress at the same strain rate under strain control. The purpose of this type test at multiple constant strain rates is to capture the effect of strain rate on the unloading stress-strain behavior. An example of the effect of the strain rate on the unloading stress-strain behavior of PMR-15 at 288 °C is presented in Figure 5.2 reproduced from McClung and Ruggles-Wrenn [6]

5.2.5 Recovery of Strain at Zero Stress. The recovery tests are preceded by loading and subsequently unloading to zero stress at multiple constant strain rates. After unloading the control mode switched from strain to load and the specimen is kept at zero load and the accumulated strain is observed until either an asymptotic solution has been reached or 100 % recovery is achieved. This setup ensured us that the specimen was no longer recovering. An example of the accumulated recovery strain preceded by loading and unloading to zero stress at multiple constant strain rate of PMR-15 at 288 °C is presented in Figure 5.3 reproduced from McClung and Ruggles-Wrenn [6]

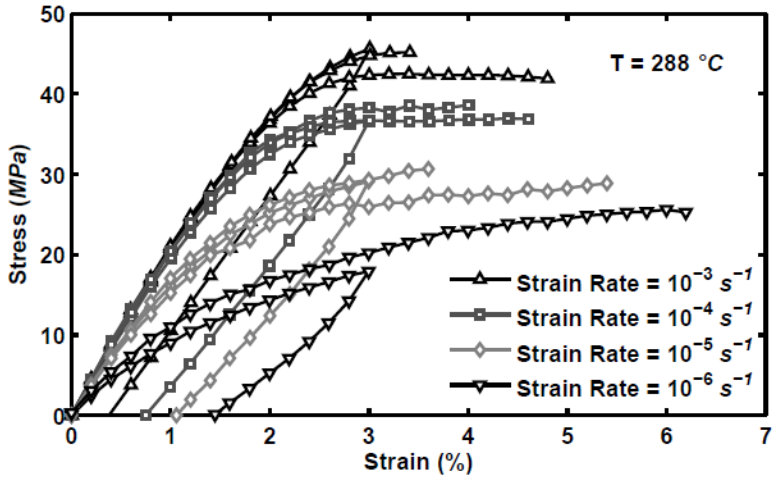

Figure 5.2: Stress-strain curves obtained for PMR-15 polymer in tensile tests to failure and in loading/unloading tests conducted at constant strain rates of 10^{-6} , 10^{-5} , 10^{-4} and 10^{-3} s^{-1} at 288 °C. The dependence of the stress-strain behavior on the strain rate is evident. Reproduced from McClung and Ruggles-Wrenn [6] Fig 2

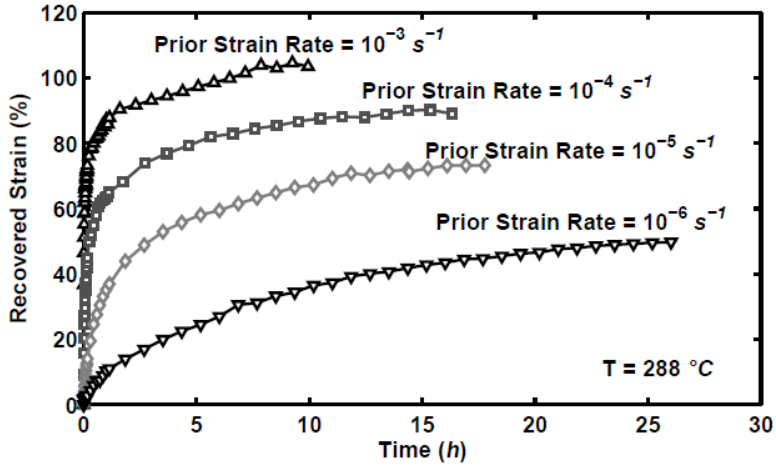

Figure 5.3: Recovery at zero stress at 288 °C following loading and unloading at constant strain rate magnitude. Recovered strain is shown as a percentage of the initial value (inelastic strain value measured immediately after reaching zero stress). The effect of the prior strain rate on the recovered strain is apparent. Reproduced from McClung and Ruggles-Wrenn [6] Fig. 3

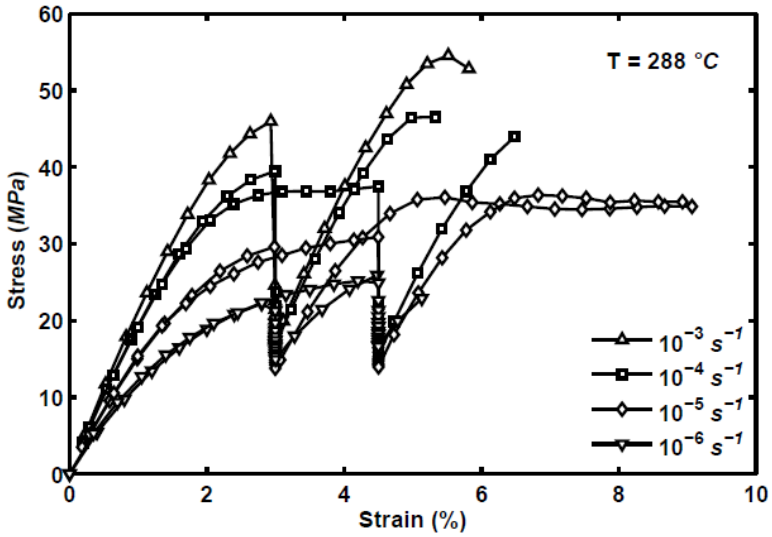

Figure 5.4: Stress-strain curves obtained for PMR-15 polymer in constant strain rate tests with intermittent periods of relaxation at 288 °C. When loading at a constant strain rate is resumed after the relaxation period, the material reaches the flow stress characteristic for that particular strain rate. Reproduced from McClung and Ruggles-Wrenn [6] Fig. 6

5.2.6 Constant Strain Rate Test with Intermittent Periods of Relaxation. Relaxation response of PMR-15 at 316 °C was explored in monotonic tests with intermittent periods of relaxation of fixed duration. In these tests, a specimen is loaded at a constant strain rate to a target strain in the region of fully established inelastic flow, where the specimen is subjected to a 12-h relaxation. After the end of the relaxation period, loading resumes at the given strain rate and continues up to failure of the specimen. The tests were conducted at the strain rates of 10^{-6} , 10^{-5} , 10^{-4} and 10^{-3} s^{-1} during both loading and relaxation under strain control by introducing a relaxation period at the strain of 4%. An example of the stress-strain behavior at multiple constant strain rates with intermittent periods of relaxation is presented in Figure 5.4 whereas the resulting stress drops are presented in Figure 5.5 of PMR-15 at 288 °C. Figures 5.4 and 5.5 are reproduced from McClung and Ruggles-Wrenn [6].

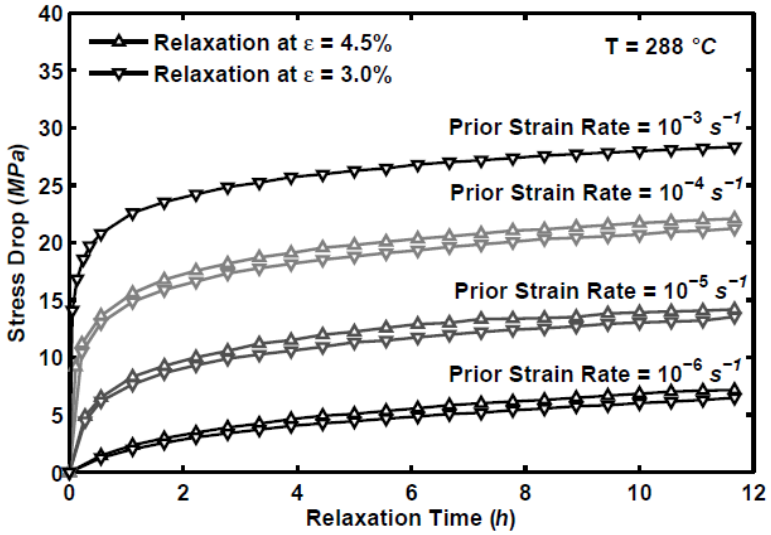

Figure 5.5: Stress decrease vs relaxation time for the PMR-15 polymer at 288 °C. Influence of prior strain rate on the stress drop during relaxation is evident. Stress drop during relaxation of a fixed duration is independent of the stress and strain at the beginning of relaxation. Reproduced from McClung and Ruggles-Wrenn [6] Fig. 7

5.2.7 Strain Rate Jump Test. The Strain Rate Jump Test (SRJT) [6,35,40] consisting of segments of monotonic loading at two different strain rates was performed to assess whether the PMR-15 polymer exhibits the strain rate history effect at 316 °C. The tests were conducted at the rates of 10^{-5} and 10^{-3} s^{-1}. An example of stress-strain behavior of PMR-15 Strain Rate Jump Test at 288 °C is presented in Figure 5.6 together with the stress-strain curves obtained in monotonic tensile tests. Figure 5.6 is reproduced from McClung and Ruggles-Wrenn [6].

5.2.8 Creep Test. The effect of the prior strain rate on creep response was studied in creep tests of 6 h duration. In these tests, a specimen is loaded to a target creep stress of 12 MPa at constant strain rates of 10^{-5} and 10^{-4} s^{-1}. The mechanical testing equipment made it possible to load the specimen to the target stress at a constant strain rate under strain control, then switch mode to load control to perform a creep test. An example of the effect of the prior strain rate on the creep

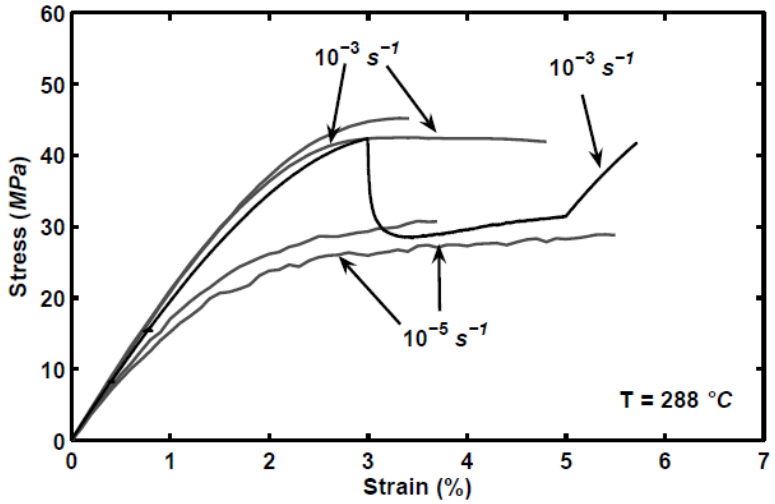

Figure 5.6: Stress-strain curves obtained for PMR-15 polymer in strain rate jump tests and in constant strain rate on a change of the strain rate, the material "returns" to the stress-strain curve characteristic for that particular strain rate. Reproduced from McClung and Ruggles-Wrenn [6] Fig. 4

behavior of PMR-15 at 288 °C is presented in Figure 5.7 reproduced from McClung and Ruggles-Wrenn [6]

5.3 Isothermal Aging

The specimens were aged in argon environment at 316 °C for durations of 50, 100, 250, 500 and 1000 h. The aging in argon was accomplished with a Blue M oven. The flow rate of the argon was approximately 20 standard cubic feet per hour (SCFH) at steady state and 200 SCFH during the purge cycle. The oven was opened without cooling and closed immediately when to remove aging samples. The oven then automatically entered the purge cycle to force out any ambient atmosphere that had entered the chamber. It is also assumed that the aging of PMR-15 at room temperature is negligible compared to those at elevated temperatures. Another important assumption is that thermal cycling of specimens during heating and cooling periods does not contribute to degradation. The number or thermal cycles is kept minimum for the sake of this assumption. These assumptions are common for the similar type of studies [9, 20].

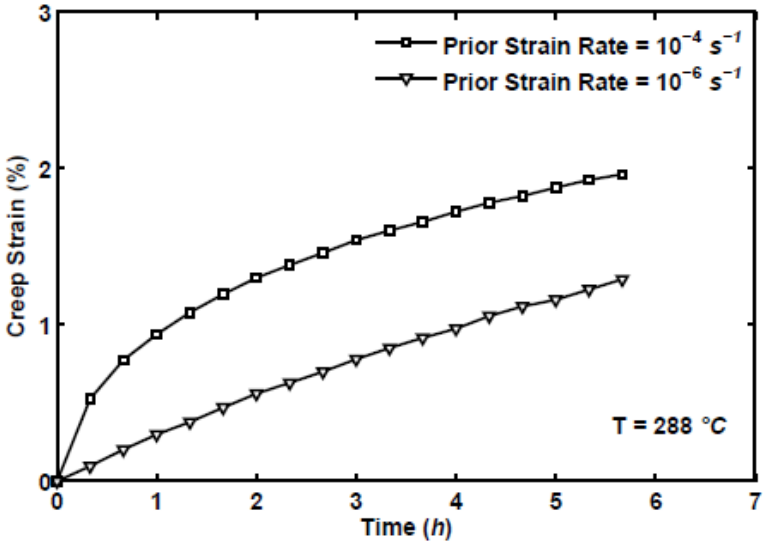

Figure 5.7: Creep strain vs time at 21 MPa and 288 °C. Effect of prior strain rate on creep is apparent. Creep strain increases nonlinearly with prior strain rate. Reproduced from McClung and Ruggles-Wrenn [6] Fig. 5

After removing the specimens from the aging chamber, they were stored in a dry-air-purged desiccator prior to mechanical testing. The desiccator was kept at a constant relative humidity of less than 10 %, to avoid the effects of moisture.

5.4 Weight Measurements

Each group of specimens subjected to a particular aging time included one rectangular blank sample in order to determine the weight loss as a function of aging time. The initial weight measurements of the blank samples were taken after drying and marking. All weight measurements were taken with a Metler Toledo AG245 microbalance with a resolution of 0.0001 grams. After aging, the blank samples were allowed to cool for a few minutes prior to weight measurements. All samples were stored in a dry-air-purged desiccator before and after aging in order to maintain near zero moisture content. The desiccator was kept at relative humidity (RH) of less than 10 % at all times.

VI. Unaged PMR-15 Neat Resin: Experimental Observations

6.1 Assessment of Specimen-to-Specimen Variability

Before aging and conducting any further testing the initial room-temperature elastic modulus of each specimen was measured in order to capture the sample to sample variability and have a foresight about each specimen. The tests were carried out at room temperature in a laboratory environment. The procedure of testing room temperature elastic modulus was discussed in section 5.2. The mean room temperature elastic modulus is 3.77 GPa. The associated standard deviation is 0.19 GPa. Although some scatter was obvious, it was decided not to eliminate any single sample based only on the room temperature elastic modulus measurement. The measured elastic modulus of each specimen has been useful for testing in reducing data scatter with respect to sample to sample variability.

6.2 Deformation Behavior at 316 °C

The test procedures described in Section 5.2 were conducted on PMR-15 neat resin with no prior thermal aging. The aim of this research is to investigate the strain rate (time)-dependent deformation behavior of the PMR-15 polymer at 316 °C. The experimental investigations includes strain-controlled tests of tension to failure, loading and unloading, monotonic loading with periods of relaxation, creep and changes in strain rate. In addition to that the effects of prior strain rate on creep behavior and also the recovery of strain at zero stress are also explored.

6.2.1 Monotonic Tension to Failure. The effect of strain rate was investigated on tension to failure tests conducted at constant strain rates of 10^{-6}, 10^{-5}, 10^{-4}, and 10^{-3} s^{-1}. The results are shown in Figure 6.1 It is observed that the stress-strain curves do not exhibit a distinct linear range and the slope of the each curve continues to decrease with increasing stress. The stress-strain curves obtained at constant strain rates of 10^{-5}, 10^{-4}, and 10^{-3} s^{-1} show little dependence on rate initially,

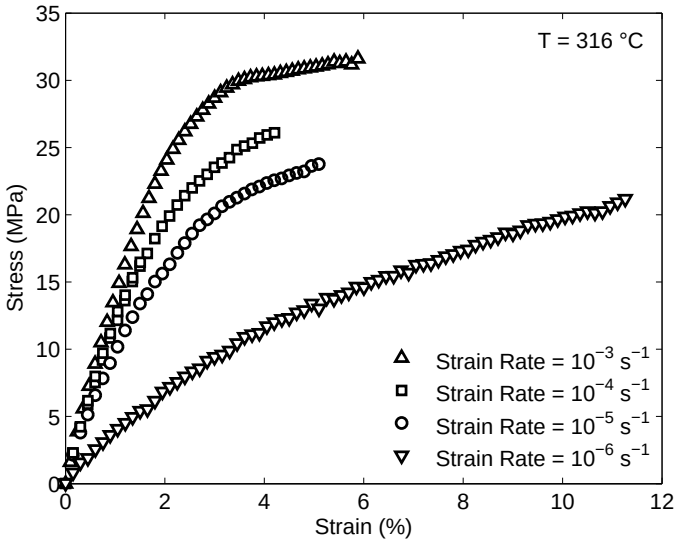

Figure 6.1: Stress-Strain Curves Obtained for PMR-15 in Tensile Test to Failure Conducted at Constant Strain Rates of 10^{-3}, 10^{-4}, 10^{-5}, and 10^{-6} s^{-1} at 316 °C. The Dependence of the Stress-Strain Behavior on the Strain Rate is Evident.

producing the same quasi-elastic slope of approximately 1.2 GPa upon leaving the origin. However with the stress-strain curve obtained at constant strain rate of 10^{-6} s^{-1}, the dependence on rate becomes more distinct, producing the quasi-elastic slope of approximately 0.5 GPa upon leaving the origin. After the transition to the inelastic regime the material exhibits positive, nonlinear strain rate sensitivity. However with the stress-strain curves obtained at constant strain rates of 10^{-5}, 10^{-4}, and 10^{-3} s^{-1} the material exhibits inability to establish inelastic flow fully and early failures are observed. The stress-strain curves obtained at slower strain rates depart from near-linear behavior at much lower stress levels than those obtained at faster strain rates. This behavior becomes much more pronounced at the constant strain rate of 10^{-6} s^{-1}. The flow stress level increases with the increasing strain rate. In addition, the shape of the stress-strain curve exhibits a gradual change as the strain rate increases. Furthermore, the "knee" of the stress-strain curve, where the quasi-linear elastic behavior transitions to inelastic flow becomes more distinct with increasing strain rate.

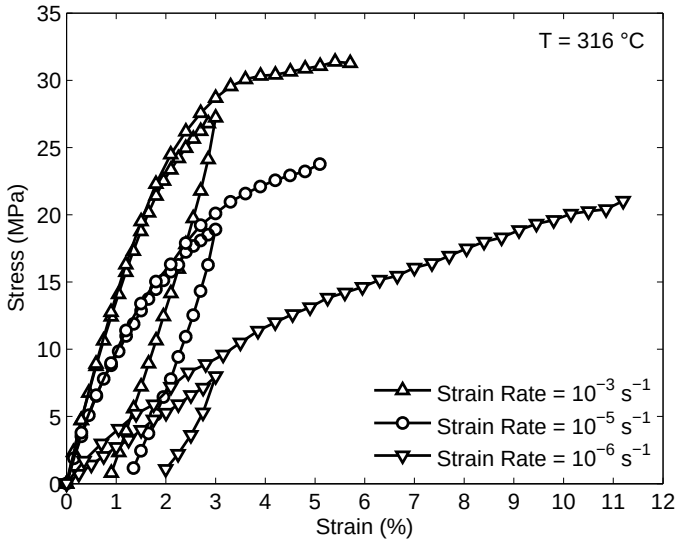

Figure 6.2: Stress-Strain Curves Obtained for PMR-15 in Loading/Unloading Tests Constant Strain Rates of 10^{-3}, 10^{-5}, and 10^{-6} s^{-1} at 316 °C Compared to Tension to Failure Results. The Dependence of the Unloading Behavior on the Strain Rate is Evident.

6.2.2 Loading and Unloading. The effect of strain rate was investigated on the unloading stress-strain behavior. The strain-controlled tests including loading to a fixed strain of 3% and unloading to zero stress at constant strain rates of 10^{-6}, 10^{-5}, and 10^{-3} s^{-1} were conducted. The results are shown in Figure 6.2. A maximum mechanical strain of 3% was selected based on tension to failure results in order to make sure that material could withstand the maximum strain at all strain rates. It is seen in Figure 6.2 that the unloading stress-strain behavior is "curved" and strongly influenced by strain rate. The curved unloading behavior becomes considerably more distinct as the strain rate decreases. The inelastic strain measured immediately after reaching zero stress increases with the decreasing strain rate.

6.2.3 Recovery of Strain at Zero Stress. Right after conducting loading and unloading to zero stress at constant strain rate, the control mode was switched from strain to load, and the load was maintained at zero stress for at least 7 h to observe the strain recovery. Results of the recovery tests are given in Figure 6.3, where

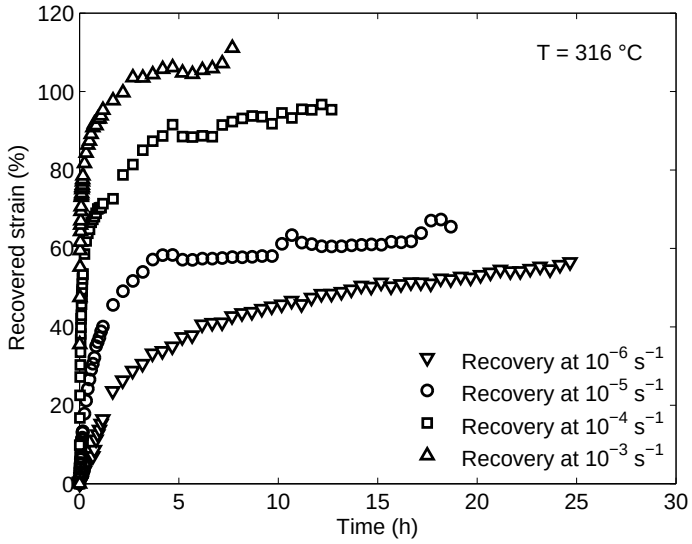

Figure 6.3: Recovery at Zero Stress at 316 °C (Following Loading and Unloading in Strain Control). Recovered Strain is Shown as a Percentage of the Initial Value (Inelastic Strain Value Measured Immediately After Reaching Zero Stress). The Effect of The Prior Strain Rate on the Recovered Strain is Apparent.

the recovered strain is shown as a percentage of the inelastic strain value measured immediately after reaching zero stress. A distinct influence of the prior strain rate on the recovery of strain is obvious. As seen in Figure 6.3 the percentage of the inelastic strain recovered increases with the increasing prior strain magnitude. The strain rate during the recovery period decreases rapidly and most of the strain is recovered after approximately 5 h for all except the slowest prior strain rate. In the test conducted with the strain rate magnitude of 10^{-3} s^{-1}, the inelastic strain measured upon unloading is fully recovered after 2 h. Conversely, in the tests conducted with slower strain rates, the inelastic strain was only partially recovered. In tests conducted with strain rate magnitudes of 10^{-4} and 10^{-5} s^{-1}, the recovery rate dropped to near zero after 10 h. Nearly 95% of the inelastic strain measured upon unloading was recovered in the 10^{-4} s^{-1} test. In the 10^{-5} s^{-1} test, 65% of the inelastic strain was recovered after 20h and approximately 55% of the inelastic strain was recovered in the 10^{-6} s^{-1} test after 25h. In the tests conducted at the strain rates of 10^{-5} and 10^{-6}

s^{-1} due to the slow rate of recovery and the strain of 69.9% and 71.4% remaining respectively at the end of the recovery period, full recovery is unlikely even given ample time. A permanent strain should be expected.

6.2.4 Monotonic Tests with Single Period of Relaxation. In these tests, a specimen is subjected to an uninterrupted loading at a constant strain rate to a target strain in the region of fully established inelastic flow, where a 12-h relaxation period is introduced. Following the relaxation period, straining resumes at the given strain rate and continues to specimen failure. The tests were conducted under strain control using strain rates of 10^{-6}, 10^{-5}, 10^{-4}, and 10^{-3} s^{-1}. In the previous research [9] by McClung revealed that only one interval of strain can be achieved within a single test, hence two relaxation periods per strain rate of interest are needed in order to evaluate the effect of the stress and strain at the beginning of relaxation on the relaxation behavior. Two relaxation periods were planned at the strain rate of 10^{-6} s^{-1} including a relaxation period at (1) the strain of 4% and (2) the strain of 5%. During the test conducted using the strain rate of 10^{-6} s^{-1} an early failure was observed right after loading to 5%. Only one relaxation period was planned including a relaxation period at the strain of 4% with the tests conducted under strain control using strain rates of 10^{-5}, 10^{-4}, and 10^{-3} s^{-1}. Results are presented in Figures 6.4 and 6.5.

It is seen in Figure 6.4 that, once the monotonic loading is resumed after the relaxation, the stress strain curve "overshoots", then it is expected to return to the stress level characteristic for a given strain rate but we can not observe such a behavior since inelastic flow is never reached before failure. The "overshoot" becomes more pronounced with the increasing strain rate and becomes hardly noticeable at strain rate of 10^{-6} s^{-1}.

Relaxation curves in Figure 6.5 reveal the effect of the prior strain rate on the stress drop. The decrease in stress during relaxation is clearly influenced by the prior strain rate. A larger decrease in stress is observed in relaxation following loading at

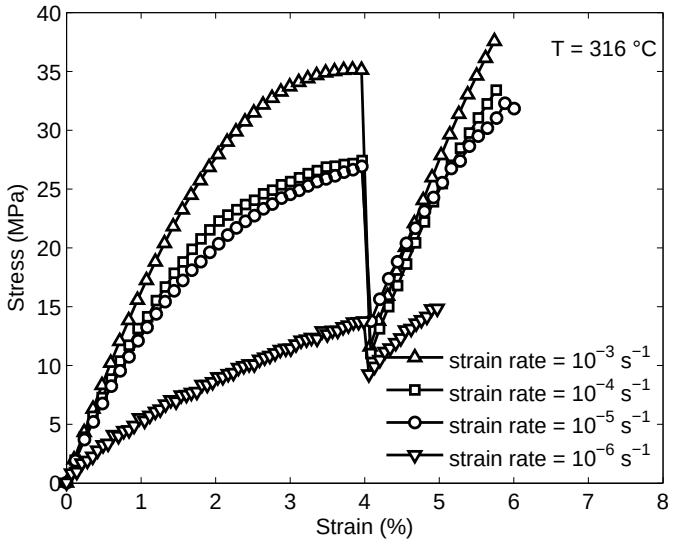

Figure 6.4: Stress-Strain Curves Obtained for PMR-15 Polymer in Constant Strain Rate Tests with a Single Period of Relaxation at 316 °C.

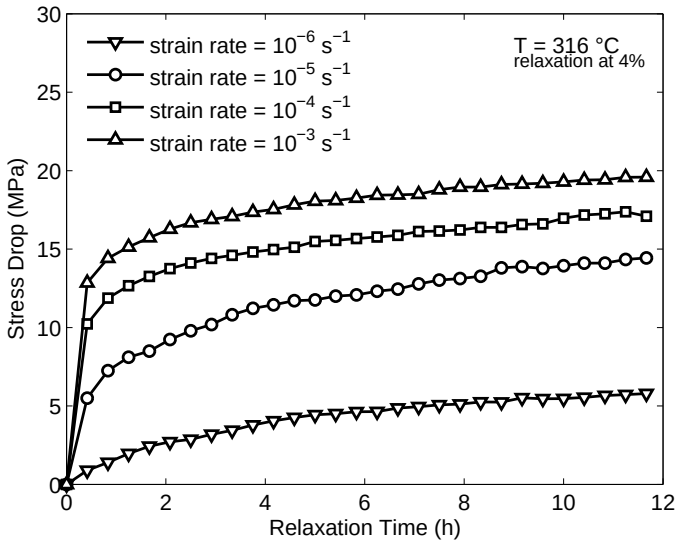

Figure 6.5: Stress Drop vs Relaxation Time for the PMR-15 Polymer at 316 °C. Influence of Prior Strain Rate on the Stress Drop during Relaxation is Evident.

10^{-3} s^{-1} than all the other strain rates. The total stress drops in the 12-h relaxation tests are increasing with increasing prior strain rate.

The results show that for relaxation periods starting at higher stress levels, the stress relaxation takes longer to saturate. In the previous research [9] by McClung it was demonstrated that it was reasonable to assume the saturation of the relaxation stress was imminent after 12 h of relaxation. It seems that the stress values at the end of the relaxation periods comes to rest which forms of a stress-strain diagram and is positioned below the stress-strain curves obtained for the slowest prior loading rate. This behavior suggests the existence of an equilibrium stress curve with the shape similar to that of the stress-strain curve obtained at 10^{-6} s^{-1}.

6.2.5 Strain Rate Jump Test. The Strain Rate Jump Test (SRJT) [35, 40] consisting of segments of monotonic loading at two different strain rates was performed to assess whether the PMR-15 polymer exhibits the strain rate history effect at 316 °C. The terminology a lack of a "strain rate history effect" used in this study is derived from definition of Krempl and his co-workers [12, 14, 35]. A material exhibits a lack of a strain rate history effect when it has a rapidly fading "memory" for the prior imposed strain rate, with the currently imposed strain rate having the most influence on the response.

In the Strain Rate Jump Test (SRJT), a specimen is subjected to an uninterrupted loading at a constant strain rate to a target strain in the region of fully established inelastic flow, where the loading rate is decreased by two orders of magnitude. This test was conducted using the strain rates of 10^{-3} and 10^{-5} s^{-1} including loading (1) to the strain of 4% and (2) to the strain of 6% respectively. After reaching 6% strain the loading is resumed using the strain rate of 10^{-3} s^{-1} until failure of the specimen. The result is presented in Figure 6.6 together with the stress strain curve obtained in constant strain rate tests conducted at the strain rates of 10^{-3} and 10^{-5} s^{-1}. The stress-strain curve obtained at 10^{-5} s^{-1} in the SRJT falls in with the stress-strain curve obtained at constant strain rate tests conducted at that strain

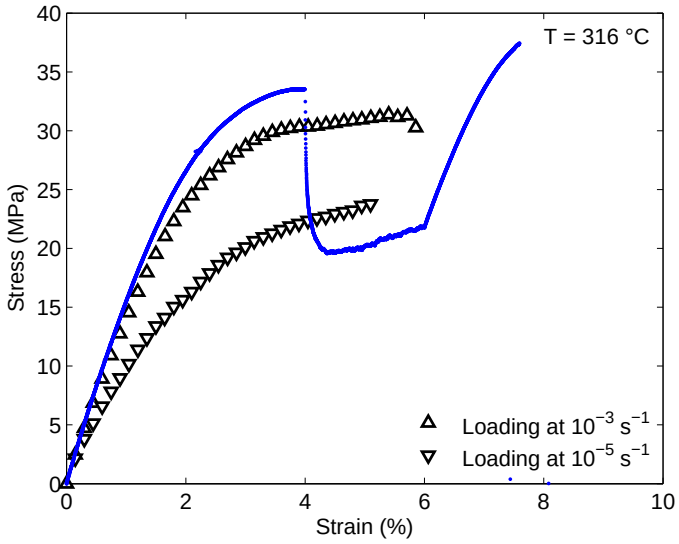

Figure 6.6: Stress-Strain Curves Obtained for PMR-15 Polymer in Strain Rate Jump Tests and in Constant Strain Rate Tests at 316 °C. Upon a Change of the Strain Rate, the Material "Returns" to the Stress- Strain Curve Characteristic for that Particular Strain Rate.

rate. As the strain rate increases from 10^{-5} to 10^{-3} s^{-1} the stress increases up to the flow stress level characteristic of that strain rate . Then it can be suggested that once the inelastic flow is fully established, a unique stress-strain curve is obtained for a given strain rate. Therefore, it can be stated that at 316 °, the PMR-15 polymer does not exhibit the strain rate history effect. The lack of a strain rate history effect in PMR-15 supports the selection of VBO as a constitutive equation.

6.2.6 Creep. The effect of the prior strain rate on creep response was studied in creep tests of 6 h duration. In these tests, a specimen is loaded to a target creep stress of 12 MPa at constant strain rates of 10^{-6}, 10^{-5} and 10^{-4} s^{-1}. The mechanical testing equipment made it possible to load the specimen to the target stress at a constant strain rate under strain control, then switch mode to load control to perform a creep test. The creep strain vs time curves are presented in Figure 6.7. Primary and secondary creep was observed in the test preceded by loading at 10^{-6}, 10^{-5} and 10^{-4} s^{-1}. It is seen in Figure 6.7 that creep behavior is strongly influenced

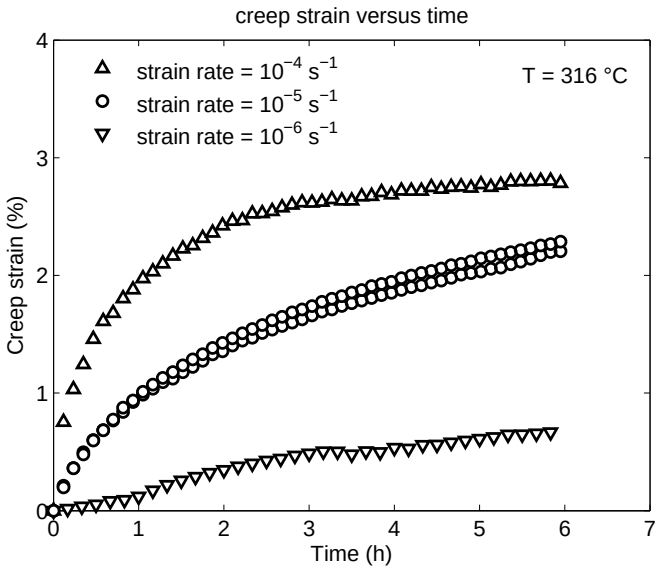

Figure 6.7: Creep Strain vs Time at 12 MPa and at 316 °C. Effect of Prior Strain Rate on Creep is Apparent. Creep Strain Increases Nonlinearly with Prior Strain Rate.

by prior strain rate. For a given stress level, creep strain accumulation increases nonlinearly with increasing prior strain rate. An increase of two orders of magnitude in prior strain rate results in a more than twofold increase in creep strain.

VII. Unaged PMR-15 Neat Resin: Constitutive Modeling and Characterization of Model Parameters

The experimental results clearly demonstrate that the PMR-15 polymer exhibits rate-dependent behavior at 316 °C. In particular the positive strain rate sensitivity during monotonic loading, the dependence of the recovery on prior unloading strain rate, the dependence of relaxation on the prior loading rate, and the lack of strain rate history effect in the strain rate jump test are observed through the experimental results. These results suggest the VBOP as a promising candidate constitutive model to represent the deformation behavior of this high-temperature polymer.

7.1 Indications For Modeling

The experimental results reported in this study reveal several key features of the deformation behavior of the unaged PMR-15 neat resin at 316 °C:

1. Linear, quasi-elastic behavior is observed upon initial loading
2. The "knee" of the stress-strain curve, where the quasi-linear elastic behavior transitions to inelastic flow becomes more distinct with increasing strain rate.
3. The unaged PMR-15 neat resin exhibits positive, nonlinear strain rate sensitivity in monotonic loading.
4. The flow stress level increases with the increasing strain rate.
5. With the stress-strain curves obtained at constant strain rates of 10^{-5}, 10^{-4}, and 10^{-3} s^{-1} in monotonic loading the transition to the inelastic flow is not observed due to early failures.
6. Once the inelastic flow is fully established, a unique stress-strain curve is obtained for a given strain rate. And it can be stated that the material does not exhibit the strain rate history effect.
7. Recovery of strain is strongly influenced by prior strain rate. The recovery rate increases with prior strain rate.

8. Creep behavior is strongly influenced by prior strain rate. For a given stress level, creep strain accumulation increases nonlinearly with increasing prior strain rate.

9. The total stress drops in the 12-h relaxation tests are increasing with increasing prior strain rate. It seems that the stress values at the end of the relaxation periods comes to rest which forms of a stress-strain diagram and is positioned below the stress-strain curves obtained at a strain rate of $10^{-6}\ s^{-1}$. This behavior suggests the existence of an equilibrium stress curve with the shape similar to that of the stress-strain curve obtained at $10^{-6}\ s^{-1}$.

It is seen that these features of the inelastic deformation behavior of the PMR-15 polymer at 316 °C are similar to the behavior exhibited at 288 °C. McClung [9] reported that the experimental results strongly suggest the usefulness of the overstress concept in the modeling inelastic deformation of the PMR-15 neat resin at 288 °C. To assess the ability of the VBOP to reproduce the essential qualitative features of the PMR-15 inelastic behavior, McClung [9] carried out several VBOP simulations and reported:

1. The VBOP simulations are consistent with the qualitative features of the inelastic behavior exhibited by the PMR-15 at 288 °C. The initial quasi-linear behavior is reproduced.

2. The positive, nonlinear rate sensitivity is also evident in monotonic loading.

3. The simulation of the stress-strain behavior in the SRJT clearly demonstrated the absence of the strain rate history effect in the VBOP simulations. The VBOP has no difficulty reproducing "the rapid forgetting" of the prior history that was observed in experiments.

4. The VBOP is capable of reproducing the effect of prior loading rate on relaxation and creep behaviors

The results presented in this study and the simulations conducted in the previous research McClung [9] show quiet consistency. Therefore once more the VBOP is

selected as a suitable choice of constitutive model to represent the inelastic behavior of the PMR-15 neat resin at 316 °C.

7.2 Review of Modeling Formulation

The chosen VBOP formulation for the PMR-15 at 316 °C is summarized in this section. The governing equation of the standard VBO is still valid [9, 36]:

$$\dot{\epsilon} = \frac{\dot{\sigma}}{E} + \frac{\sigma - g}{Ek} \tag{7.1}$$

The growth law for the equilibrium stress is [9]:

$$\dot{g} = \Psi \frac{\dot{\sigma}}{E} + \frac{\Psi}{E}\left[\frac{(\sigma - g)}{k} - \frac{(g - f)}{A}\left|\frac{(\sigma - g)}{k}\right|\right] + \left(1 - \frac{\Psi}{E}\right)\dot{f} \tag{7.2}$$

The evolution of the kinematic stress takes the form [9]:

$$\dot{f} = \left(\frac{|\sigma|}{\Gamma + |g|}\right) E_t \left(\frac{\sigma - g}{Ek}\right) \tag{7.3}$$

The term Γ stands for the overstress invariant, and it has the form:

$$\Gamma = |\sigma - g| \tag{7.4}$$

The evolution of the isotropic stress [9] retains the form as in the VBO:

$$\dot{A} = A_c[A_f - A]\left|\frac{\sigma - g}{Ek}\right| \tag{7.5}$$

In the case of PMR-15 at 316 °C, this is simplified by setting $A_c = 0$ and making A constant as in the case of PMR-15 at 288 °C in reference [9]

The recommended basic form for the shape function is given as [9]:

$$\Psi = C_1 + (C_2 - C_1)e^{-C_3|\epsilon^{in}|} \tag{7.6}$$

where C_1, C_2, and C_3 are material constants.

The basic form of the viscosity function [9] is:

$$k = k_1 \left(1 + \frac{|\sigma - g|}{k_2}\right)^{-k_3} \tag{7.7}$$

where k_1, k_2, and k_3 are material constants.

The specific form of each equation was chosen based on the mechanical behavior observed in the experiments of the PMR-15 at 316 °C described in Chapter VI and the model characterization process proposed by McClung [9].

7.3 Model Characterization Procedure

It is critical to estimate the nine constants in VBOP from experimental data in order to obtain a well-developed model that captures the material behavior. To develop a systematic characterization scheme for VBOP is beyond the objective of this effort. Instead the model characterization process that was proposed by McClung [9] for PMR-15 at 288 °C was used for the case of PMR-15 at 316 °C.

The proposed model characterization procedure was described by McClung [9] as follows:

1. Determine elastic modulus and tangent modulus from monotonic tensile data.
2. Determine the equilibrium stress from relaxation data.
3. Determine the isotropic stress from the equilibrium stress and the tangent modulus.
4. Assess the viscosity function using results of the relaxation tests conducted with various prior strain rates. Least squares optimization can be used to match

Table 7.1: Material Parameters Used in the VBOP Predictions of the Deformation Behavior of the Unaged PMR-15 Neat Resin at 316 °C.

Function	Parameters
Moduli	$E = 1620$ MPa, $E_t = 90$ Mpa
Isotropic Stress	$A = 9.4$ MPa
Viscosity Function	$k_1 = 1.2e4$ s, $k_2 = 33$ MPa, $k_3 = 14$
Shape Function	$C_1 = 100$ MPa, $C_2 = 500$ MPa, $C_3 = 10$

experimental data. This optimization does require seed values for the shape function parameters.

5. Determine the shape function parameters from stress-strain curves obtained in loading tests. Least squares optimization can be used to match experimental data.

6. If an unacceptable discrepancy exists in the simulations vs the experimental data for the set of loading histories in interest, reassess the particular VBOP formulation chosen to model the material behavior.

The elastic modulus E and the tangent modulus E_t are respectively easy to determine as the slopes (measured in the appropriate regions) of the tensile stress-strain diagram at the initial loading and at the maximum strain of interest, respectively. The isotropic stress can be determined once the equilibrium stress is known. However, the viscosity function parameters and the shape function parameters are estimated by a "guess-and-check" method of matching simulations to experimental data.

The following discussion summarizes the adopted model characterization procedure, which has been validated using the experimental results obtained for the PMR-15 neat resin. The model parameters obtained with the adopted characterization procedure for the PMR-15 at 316 °C are summarized in Table 7.1.

The model parameters for the case of the PMR-15 at 288 °C are summarized in Table 7.2 reproduced from McClung [9]

Table 7.2: Material Parameters Used in the VBOP Predictions of the Deformation Behavior of the Unaged PMR-15 Neat Resin at 288 °C.

Function	Parameters
Moduli	$E = 2080$ MPa, $E_t = 18$ Mpa
Isotropic Stress	$A = 20$ MPa
Viscosity Function	$k_1 = 1.0e4$ s, $k_2 = 35$ MPa, $k_3 = 12$
Shape Function	$C_1 = 100$ MPa, $C_2 = 1.0e3$ MPa, $C_3 = 10$

7.3.1 Elastic Modulus and Tangent Modulus. Inelastic flow is established once the stress is sufficiently beyond the elastic region and when the tangent modulus is much smaller than the elastic modulus. This region is called "flow stress" The elastic modulus is determined from the initial quasi-linear region of the tensile stress-strain curve. The tangent modulus, defined as the slope of the stress-strain curve at the maximum strain of interest, is determined from the flow stress considerably past the "knee" of the stress-strain diagram, where inelastic flow is fully established. Tension to Failure tests in monotonic loading were used in order to determine the elastic and tangent moduli. The elastic modulus was obtained using Tension to Failure tests in monotonic loading at the rate of 10^{-3} s^{-1} and was determined as $E = 1.62$ GPa. The tangent modulus was obtained using Tension to Failure tests in monotonic loading at the rate of 10^{-5} s^{-1} and was determined as $E_t = 90$ MPa.

7.3.2 Equilibrium Stress and Isotropic Stress. Results of the constant strain rate tests with periods of relaxation at the strain of 4% were used to determine the equilibrium stress. It was stated before that the relaxation periods comes to rest which forms of a stress-strain diagram and is positioned below the stress-strain curves obtained for the slowest prior loading rate. The equilibrium stress was estimated as 13 MPa from the experimental results. This value of the equilibrium stress at the strain of 4% was used to determine the isotropic stress from;

$$A = g - E_t \epsilon \tag{7.8}$$

where the brackets n designate the asymptotic limit of n [9]. The isotropic stress was determined as $A = 9.4$ MPa

7.3.3 Viscosity Function. The viscosity function k controls the rate-dependence. The material parameters k_1, k_2, and k_3 of the viscosity function are estimated from the results of the relaxation tests conducted with the strain rates of 10^{-6}, 10^{-5}, 10^{-4} and 10^{-3} s^{-1}. For the unaged PMR-15 neat resin, the parameters of the viscosity function were estimated using the least squares optimization routine in MATLAB to fit to the VBOP simulations to the experimental stress values in the last two hours of the relaxation periods. The MATLAB code developed by McClung [9] was used for this optimization process. It can be seen in the Figure 6.5 where the stress drop vs time was plotted, the magnitude of the stress drops with the prior strain rate of 10^{-5}, 10^{-4} and 10^{-3} s^{-1} were close to each other respectively to the 10^{-6}. Therefore the optimization process was modified in a way that optimization took place among the strain rates of 10^{-5}, 10^{-4} and 10^{-3} s^{-1} since it was easier to model the slowest strain rate respectively to the other rates. The parameters of the viscosity function were found to be $k_1 = 1.2e + 04$ s, $k_2 = 33$ MPa, and $k_3 = 14$. The numerical simulations of the stress-time behavior during relaxation periods at 4% strain with prior loading at 10^{-6}, 10^{-5}, 10^{-4} and 10^{-3} s^{-1} generated using these values of k_1, k_2, and k_3 are shown in Figure 7.1. In terms of the prior strain rates of 10^{-6} and 10^{-4} s^{-1}, the effect of the prior strain rate on stress response is captured well. The scatter within the experimental data is approximately 1 MPa for the prior strain rates of 10^{-6} and 10^{-4} s^{-1}. For the case of the strain rate 10^{-3} s^{-1} the numerical results slightly over predict the stress drop in the early stages of relaxation. However, after approximately 6 h of relaxation time, the predictions and the experimental results begin to merge together. For the case of the strain rate 10^{-5} s^{-1} the numerical results slightly under predict the stress drop in the final stages of relaxation. After approximately 6 h of relaxation time, the predictions and the experimental results begin to diverge from each other. (At approximately 6 h of relaxation time the error between the experimental stress

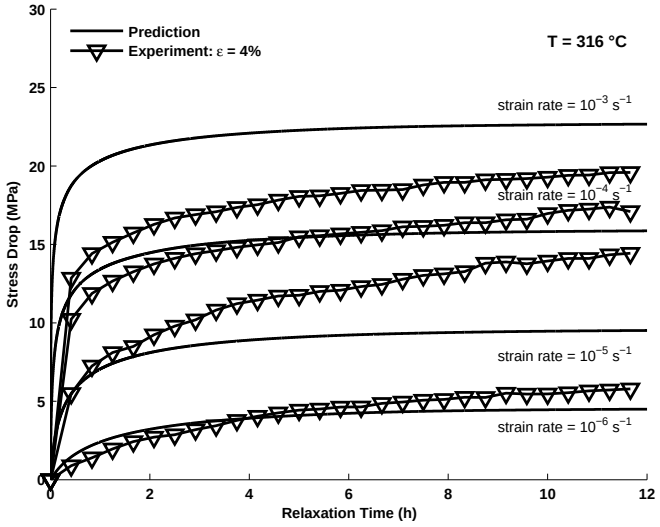

Figure 7.1: A Comparison Between Experimental and Predicted Stress Decrease vs Relaxation Time for the PMR-15 Polymer at 316 °C. Influence of Prior Strain Rate on the Stress Drop During Relaxation is Evident. The Model Successfully Represents the Stress Drop During Relaxation.

drop and the simulated stress drop is less than 3 MPa and continuously increasing and at approximately 12 h of relaxation time is reaching to 3 MPa). This discrepancy with the prior strain rate of 10^{-5} s^{-1} was referred to the scatter in the experimental data. Overall, the fit is an appropriate choice within the power law shape of the viscosity formulation. The influence of prior strain rate on stress response in relaxation is captured well in the simulation.

7.3.4 Shape Function. The shape function controls the shape of the "knee" in the stress-strain diagram in monotonic loading and also the curvature of the unloading stress-strain curve. The results of the Tension to Failure tests in monotonic loading were used in a least square optimization in MATLAB to determine the parameters C_1, C_2, and C_3 of the shape function.

The predictions of the tension to failure behavior of the PMR-15 at 316 °C are shown in Figure 7.2. The resulting model gave a good representation of the experimental data except for a slight over prediction of stress in the "knee" of the stress-strain

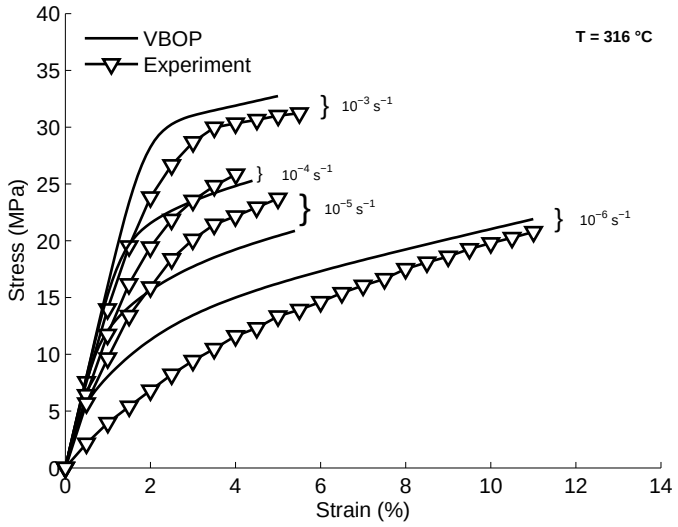

Figure 7.2: A Comparison Between Experimental and Predicted Stress-Strain Curves Obtained for PMR-15 Polymer at Constant Strain Rates of 10^{-6}, 10^{-5}, 10^{-4}, and 10^{-3} s^{-1} at 316 °C

curve at the strain rate of 10^{-6} s^{-1}. While the maximum scatter within the experimental data at this strain rate is 4 MPa at 3% strain, it is continuously decreasing and emerging quickly at 6% strain. Also there exists a slight under estimation of stress at the strain rate of 10^{-5} s^{-1}. The maximum scatter within the experimental data at this strain rate is 3 MPa, while the difference between the simulations and the experimental data is within 4 MPa. The shape function parameters obtained for PMR-15 are shown in Table 7.1.

7.4 Model Verification

The characterization procedure and the resulting material parameters are validated by comparing model predictions with the experimental results. In order to verify the validity of the characterization procedure, predictions of experiments that were not utilized in the characterization process were carried out. These predictions include the strain rate jump test, loading and unloading in strain control, and creep test with varying prior strain rate.

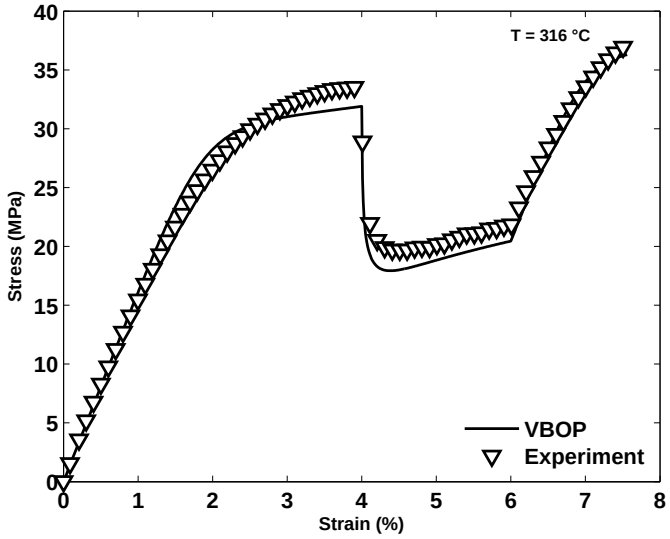

Figure 7.3: A Comparison Between Experimental and Predicted Stress-Strain Curves Obtained for PMR-15 Polymer in the Strain Rate Jump Test at 316 °C. The Model Successfully Represents the Behavior Upon a Change in Strain Rate.

Simulation of the strain rate jump test, conducted with the strain rates of 10^{-3} and 10^{-5} s^{-1}, is demonstrated together with the experimental data in Figure 7.3. Good agreement with the experimental data is observed during loading at 10^{-3} s^{-1} and during loading at 10^{-5} s^{-1} and as well as during the second period of loading at 10^{-3} s^{-1}. The VBOP predictions are within 2 MPa of the experimental results.

The predictions of loading and unloading with the strain rates of 10^{-5} and 10^{-3} s^{-1} are shown in Figure 7.4. The model does not capture the unloading stress-strain behavior at all the strain rates with the desired accuracy. However, the model captures the influence of the prior strain rate on the unloading stress-strain behavior and the increased curvature of the unloading stress-strain curves observed for the slowest strain rate.

The influence of the prior strain rate on creep behavior was examined in creep tests of 6 h duration preceded by uninterrupted loading to a target creep stress of 12 MPa at 10^{-6} and 10^{-5} s^{-1}. It is seen in Figure 7.5 that the creep strain increases nonlinearly with prior loading rate.

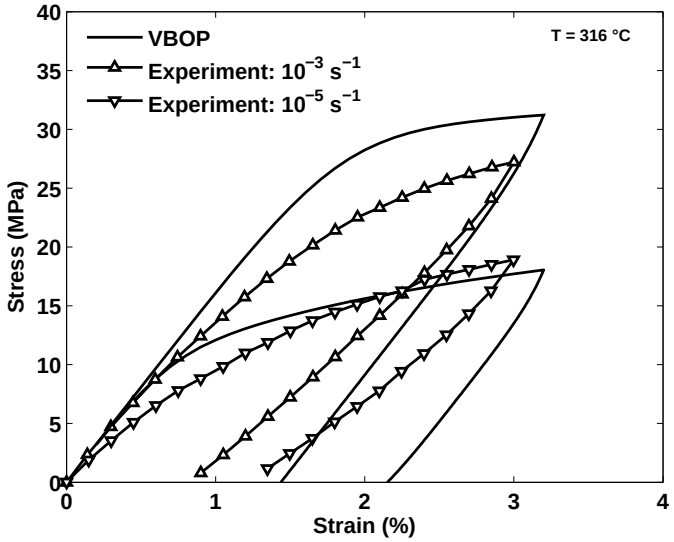

Figure 7.4: A Comparison Between Experimental and Predicted Stress-Strain Curves Obtained for PMR-15 Polymer in Loading and Unloading at Two Constant Strain Rates at 316 °C. The Model Successfully Represents the Strain Rate Dependence on the Unloading.

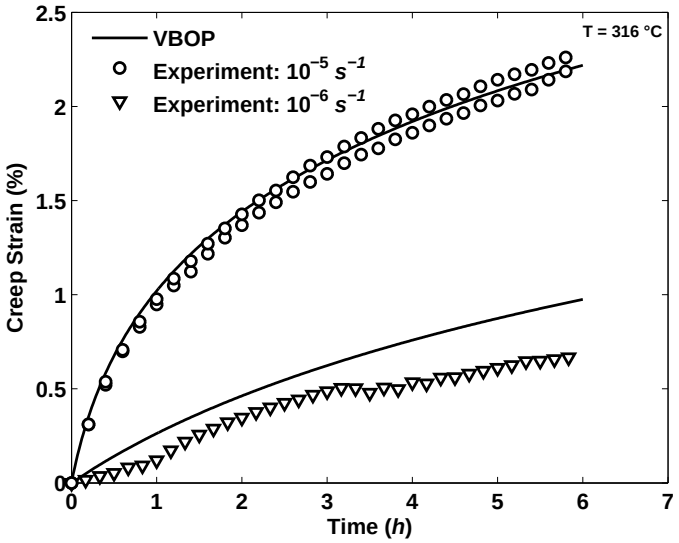

Figure 7.5: Comparison Between the Experimental and Predicted Strain vs Time Curves Obtained for PMR-15 Polymer at 316 °C in Creep at 12 MPa. Prior Loading at Strain Rates of 10^{-6} and 10^{-5} s^{-1}.

The experimental results needed to characterize the VBOP parameters were evaluated in this effort. The model capabilities were evaluated by comparing the model predictions with the experimental results obtained in tests that were not utilized in model characterization. Excluding the unloading simulations, the predictions of the material response are in good agreement with the experimental data.

VIII. Aged PMR-15 Neat Resin: Experimental Observations

The objective of this chapter is to discuss the effect of prior thermal aging at 316 °C in argon on the strain rate-dependent mechanical behavior of the PMR-15 neat resin at 316 °C. Specimens were aged following the methods outlined in Section 5.3.

8.1 Assessment of Specimen-to-Specimen Variability

The room temperature elastic modulus measurements discussed in Section 6.1 was conducted before any aging procedures started. So the discussion in Section 6.1 included the room temperature elastic modulus measurements for the aged specimens.

8.2 Weight Loss Measurements

The weight of samples aged for particular times in argon was measured. The weight measurement procedure was discussed in section 5.4. Some small magnitude of weight loss was observed. In previous studies [20, 22] the weight loss has been attributed to the loss of low molecular weight particles as the polymer is degraded by the temperature over time. Figure 8.1 compares the current effort to the previous effort [20] and shows percent weight loss for PMR-15 Neat Resin Aged in Argon at 316 °C and 288 °C respectively as a function of aging time.

8.3 Strain Controlled Tension to Failure Tests in Monotonic Loading

Specimens from each aging group discussed in section 5.3 were subjected to strain-controlled tension-to-failure tests at constant strain rates of 10^{-6}, 10^{-5}, 10^{-4}, and 10^{-3} s^{-1}. Previous work [6, 9] has shown that the PMR-15 polymer exhibits strain rate dependent behavior during monotonic loading.

The results of the strain controlled tension-to-failure tests for PMR-15 specimens aged in argon for 50 h Figure 8.2 show that the influence of the strain rate on the stress-strain behavior is evident. It is noteworthy that the stress strain curves in Figure 8.2 do not exhibit a truly linear range upon leaving the origin. The stress-strain curves obtained at different strain rates for the specimens aged in argon for

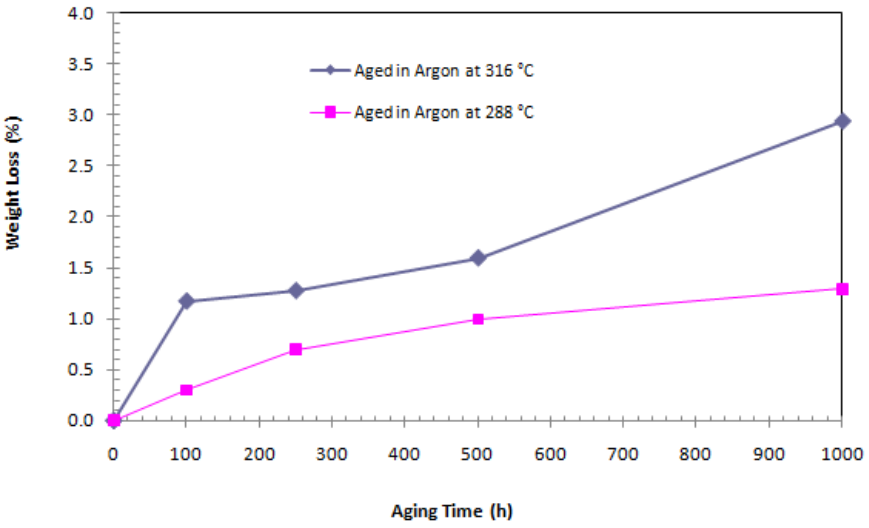

Figure 8.1: Comparison of Percent Weight Loss for Pmr-15 Neat Resin Aged in Argon at 316 °C and 288 °C

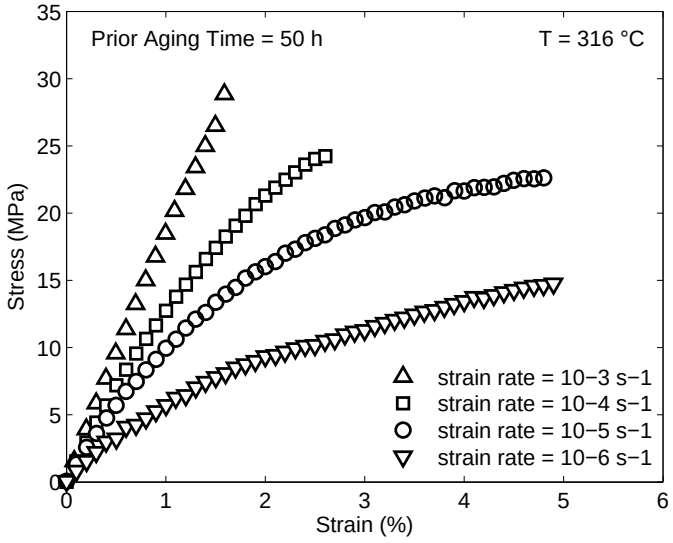

Figure 8.2: Stress-Strain Curves for PMR-15 Specimens Aged for 50 h at 316 °C in Argon Obtained in Tensile Tests to Failure Conducted at Constant Strain Rates of 10^{-6}, 10^{-5}, 10^{-4}, and 10^{-3} s^{-1} at 316 °C. The Dependence of the Stress-Strain Behavior on the Strain Rate is Evident.

50 h do however exhibit the same quasi-elastic slope upon leaving the origin. In addition the stress-strain curves obtained at slower strain rates depart from linearity at a much lower stress level than those obtained at faster strain rates. The shape of the stress-strain curve undergoes a gradual change as the strain rate increases. The transition from the initial quasi-elastic behavior to inelastic regime is not observed at higher strain rates. There exist early failures for the strain rates 10^{-4} and 10^{-3} s^{-1}. For the strain rates 10^{-6} and 10^{-5} s^{-1}, after the transition from the initial quasi-elastic behavior to the inelastic regime, the material exhibits normal positive strain rate sensitivity. The flow stress level increases with increasing strain rate. However, the results of the tension-to-failure tests for PMR-15 specimens aged in argon for 100 h, up to 1000 h in Figures 8.3, 8.4, 8.5 and 8.6 show that the influence of the strain rate on the stress-strain behavior is no longer observed. As the prior aging duration increases the effect of the strain rate on the stress-strain behavior is not observed. Of specific interest, at slower rates diverging from linearity at a much lower stress level and positive rate sensitivity is not observed anymore. The shape of the stress-strain curve does not undergo a gradual change and the relation between the flow stress and the increasing stress level does not exist. In addition transition to inelastic flow is no longer observed. The specimens, which are subjected to prior aging in argon for more than 50 h, exhibit only quasi-linear behavior until failure.

The stress-strain response of specimens aged in argon for durations up to 1000 h obtained during strain-controlled tension to failure tests at the rates of 10^{-6}, 10^{-5}, 10^{-4} and 10^{-3} s^{-1} is presented in Figures 8.7, 8.8, 8.9 and 8.10. It is seen that prior aging in argon does affect the stress-strain behavior of the material for all strain rates. No data can be shown for the influence of the prior aging on the departure from the quasi-linear behavior, on the initial and the final slope of the stress strain curve and on the flow stress level as well as shape of the stress-strain curve for the tests conducted with any of the prior strain rates. The material subjected to prior aging for durations up to 1000 h exhibited only quasi-linear behavior until failure.

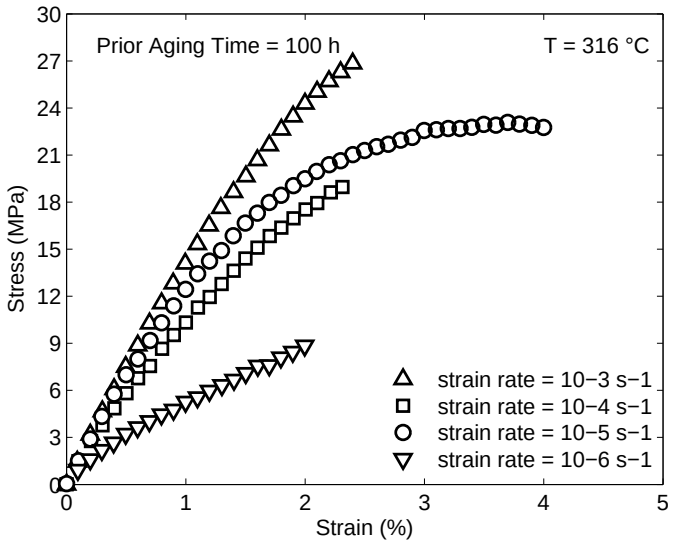

Figure 8.3: Stress-Strain Curves for PMR-15 Specimens Aged for 100 h at 316 °C in Argon Obtained in Tensile Tests to Failure Conducted at Constant Strain Rates of 10^{-6}, 10^{-5}, 10^{-4}, and 10^{-3} s^{-1} at 316 °C.

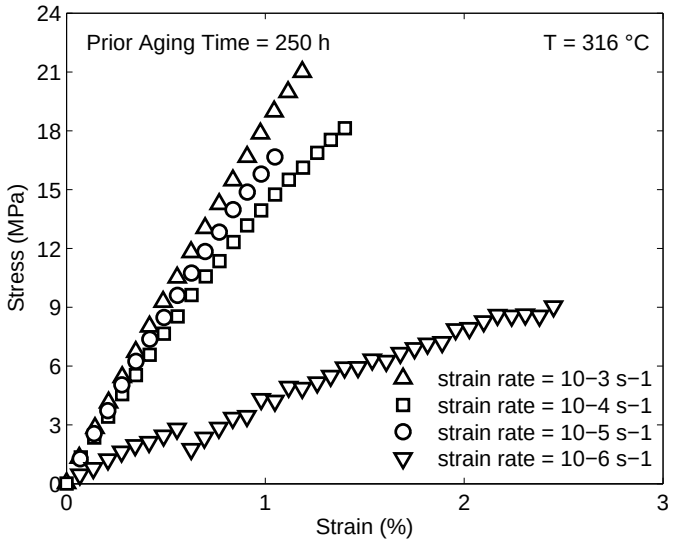

Figure 8.4: Stress-Strain Curves for PMR-15 Specimens Aged for 250 h at 316 °C in Argon Obtained in Tensile Tests to Failure Conducted at Constant Strain Rates of 10^{-6}, 10^{-5}, 10^{-4}, and 10^{-3} s^{-1} at 316 °C.

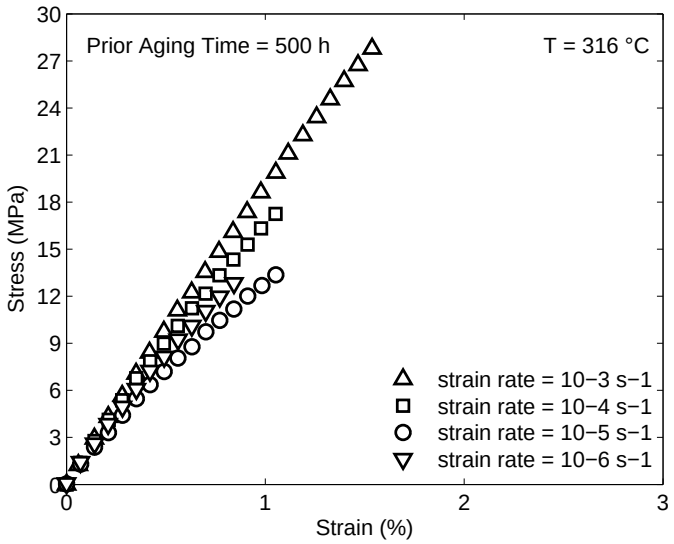

Figure 8.5: Stress-Strain Curves for PMR-15 Specimens Aged for 500 h at 316 °C in Argon Obtained in Tensile Tests to Failure Conducted at Constant Strain Rates of 10^{-6}, 10^{-5}, 10^{-4}, and 10^{-3} s^{-1} at 316 °C.

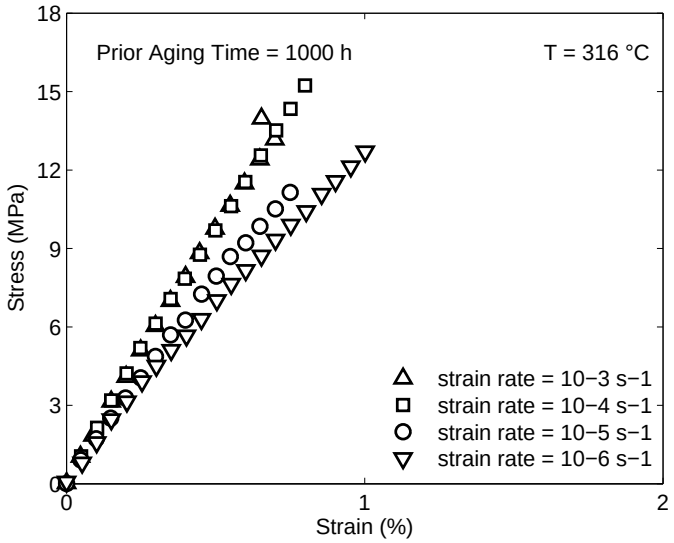

Figure 8.6: Stress-Strain Curves for PMR-15 Specimens Aged for 1000 h at 316 °C in Argon Obtained in Tensile Tests to Failure Conducted at Constant Strain Rates of 10^{-6}, 10^{-5}, 10^{-4}, and 10^{-3} s^{-1} at 316 °C.

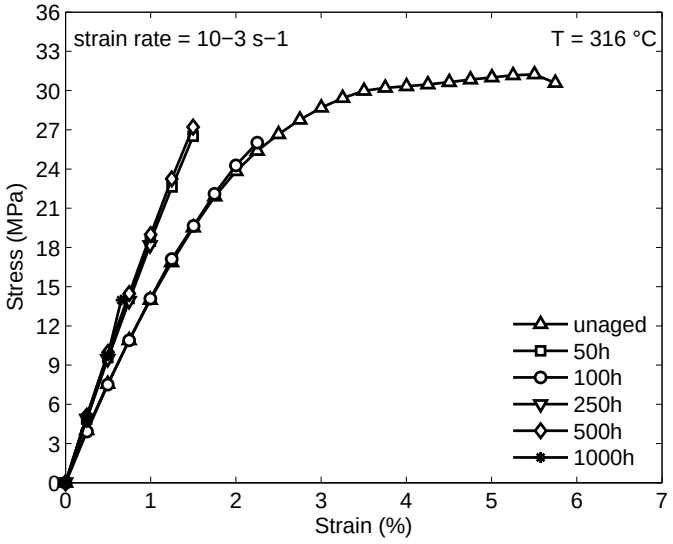

Figure 8.7: Stress-Strain Curves for PMR-15 Specimens Aged at 316 °C in Argon Obtained in Tensile Tests to Failure Conducted at Constant Strain Rate of 10^{-3} s^{-1}.

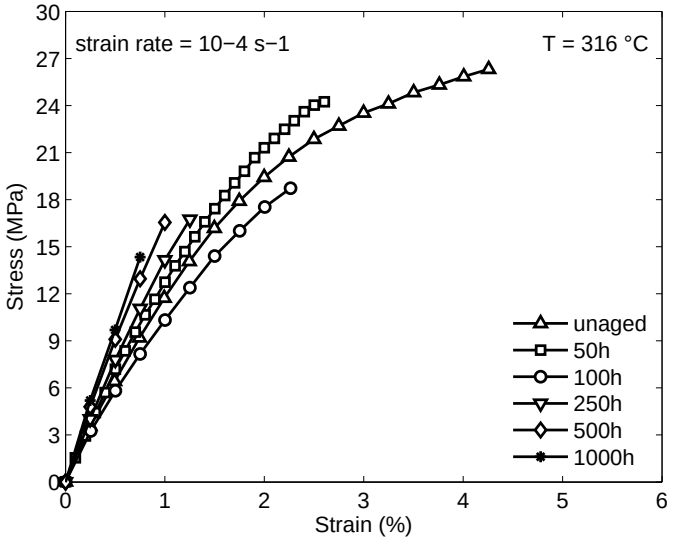

Figure 8.8: Stress-Strain Curves for PMR-15 Specimens Aged at 316 °C in Argon Obtained in Tensile Tests to Failure Conducted at Constant Strain Rate of 10^{-4} s^{-1}.

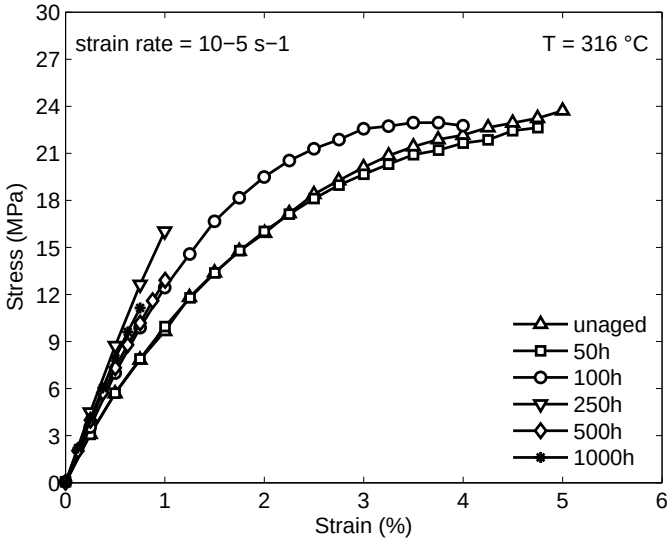

Figure 8.9: Stress-Strain Curves for PMR-15 Specimens Aged at 316 °C in Argon Obtained in Tensile Tests to Failure Conducted at Constant Strain Rate of 10^{-5} s^{-1}.

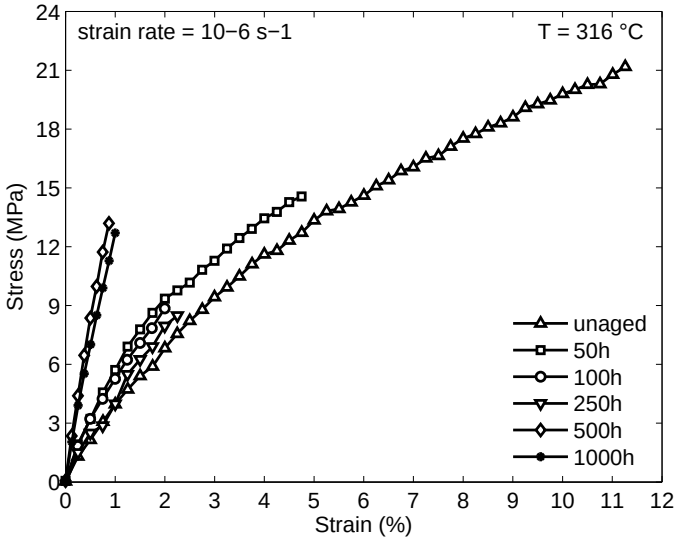

Figure 8.10: Stress-Strain Curves for PMR-15 Specimens Aged at 316 °C in Argon Obtained in Tensile Tests to Failure Conducted at Constant Strain Rate of 10^{-6} s^{-1}.

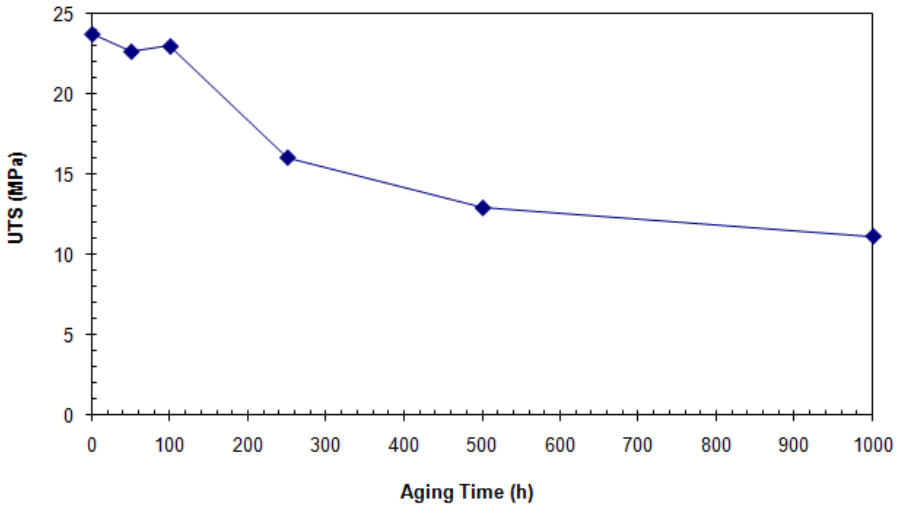

Figure 8.11: UTS at 316 °C vs Prior Aging Time for the PMR-15 Neat Resin Specimens Aged at 316 °C in Argon. UTS Decreases with Prior Aging Time.

Finally, for aging durations above 50 h, the material shows a decreasing capacity for inelastic straining with increasing prior aging time. This observation is made at all strain rates in the 10^{-6} to 10^{-3} s^{-1} range. The specimens aged over 50 h show an inability to strain past the region of quasi-elastic behavior at strain rates of 10^{-6}, 10^{-5}, 10^{-4}, and 10^{-3} s^{-1}, as shown in Figures 8.3, 8.4, 8.5 and 8.6. In addition to the reduced capacity for inelastic straining, the material shows a reduction in strength for aging durations above 100 h. The change in UTS vs aging time at the strain rate 10^{-5} s^{-1} is shown in Figure 8.11. The material exhibits ultimate tensile strengths (UTS) of 22 to 23 MPa when subjected to prior aging up to 100 h. However, the material aged for 500 h shows an UTS of 13 MPa and the material aged for 1000 h shows an UTS of 11 MPa.

8.4 Summary of the Key Effects of Prior Aging on Deformation Behavior

It has been demonstrated in this chapter that the prior thermal aging in argon does influence the mechanical behavior of the PMR-15 at 316 °C. The key features of material behavior at 288 °C that depend on prior aging time were stated in the previous effort by McClung [9] as follows:

- Initial slope of the stress-strain curve (elastic modulus) increases with increasing aging time.
- Final slope of the stress-strain curve (tangent modulus) increases with increasing aging time.
- Flow stress increases with increasing aging time.
- Departure from quasi-linear behavior is delayed with increasing aging time.

In the case of PMR-15 at 316 °C these results was not observed over 50 h duration aging time. The specimens, which are subjected to prior aging in argon for more than 50 h, exhibit only quasi-linear behavior until failure. In addition transition to inelastic flow is no longer observed. The specimens aged over 50 h show an inability to strain past the region of quasi-elastic behavior at strain rates of 10^{-6}, 10^{-5}, 10^{-4}, and 10^{-3} s^{-1}. In addition to the reduced capacity for inelastic straining, the material shows a reduction in strength for aging durations above 100 h. And there exists early failures. Based on these experimental observations, modeling the deformation behavior of PMR-15 neat resin subjected to prior aging at 316 °C is no longer area of interest since material is not behaving.

IX. Overshooting the Test Temperature

This effort investigates the deformation behavior of PMR-15 neat resin at 316 °C. In the previous effort [20] it was reported that the unaged PMR-15 neat resin found to have a T_g of 331 °C. Therefore, it was easy to overshoot the test temperature. Figures 9.1, 9.2, 9.3, 9.4 and 9.5 depicts this overshooting problem. Subsequently the real experimental data and the overshooting data are compared.

It is seen that in the case of overshooting 316 °C, after the transition to the inelastic regime the material still exhibits positive, nonlinear strain rate sensitivity. Although the material still exhibits inability to establish inelastic flow fully and early failures are observed at higher strain rates when compared to the real experiment data the transition to inelastic regime is more likely. The increasing of the flow stress level with increasing strain rate is still observed. While an increased capacity for inelastic straining is obvious, the material shows a reduction in strength. Likewise, a reduction in strength is profoundly exhibited in Monotonic Loading and Unloading Tests. It is consistent with the experimental data at 316 °C that the unloading stress-strain behavior is "curved" and strongly influenced by strain rate.

It is seen in Figure 9.3 that a reduction in strength is profoundly exhibited in Monotonic Loading with Single Period of Relaxation. Once the loading is resumed stress strain curves overshoots the initial flow stress level. The overshooting is more pronounced when compared to those at 316 °C. Relaxation curves in Figure 9.4 reveal the effect of the temperature on the stress drop while the effect of the prior strain rate observed is similar. The decrease in stress drops during relaxation is clearly influenced by the test temperature. A larger decrease in stress is observed in relaxation following loading with all the strain rates at 316 °C.

The results obtained in the SRJT falls in with the results obtained at 316 °C. Once the inelastic flow is fully established, a unique stress-strain curve is obtained for a given strain rate. The PMR-15 polymer still does not exhibit the strain rate history effect at this temperature.

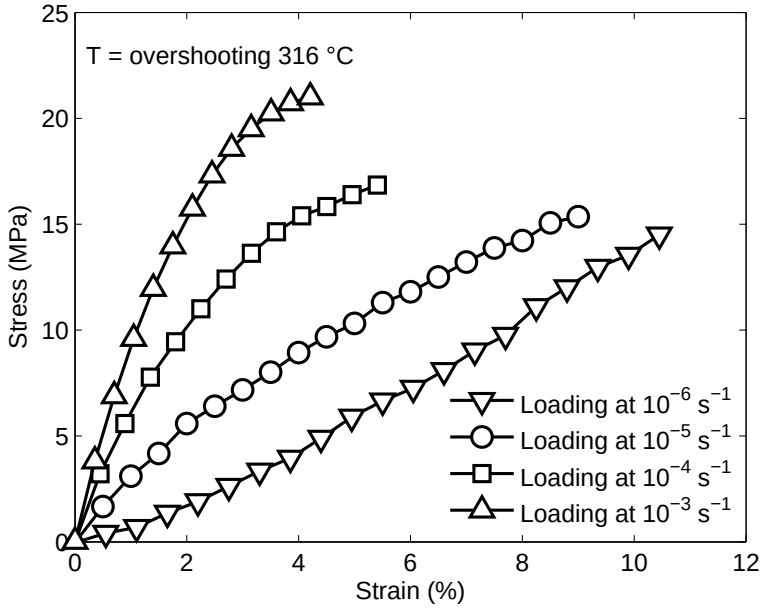

Figure 9.1: Overshooting the Test Temperature of 316 °C. The results of the Tension to Failure Tests in Monotonic Loading are exhibited.

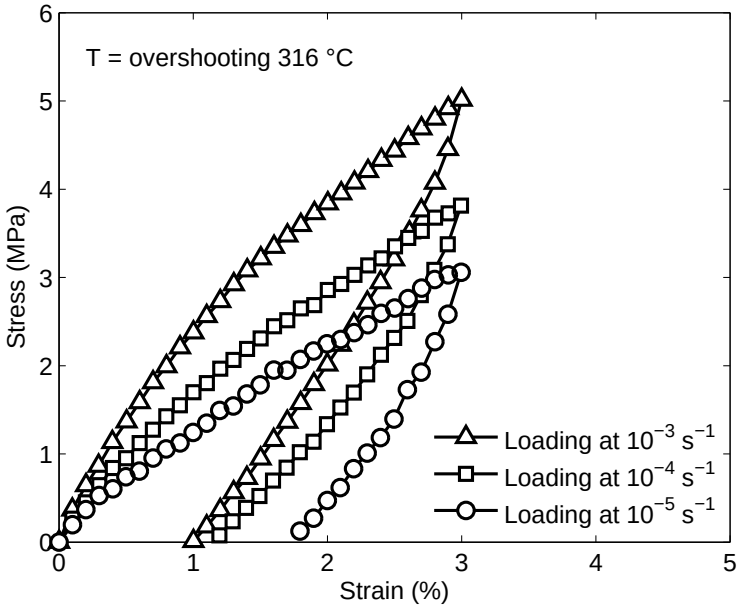

Figure 9.2: Overshooting the Test Temperature of 316 °C. The results of the Monotonic Loading and Unloading are exhibited.

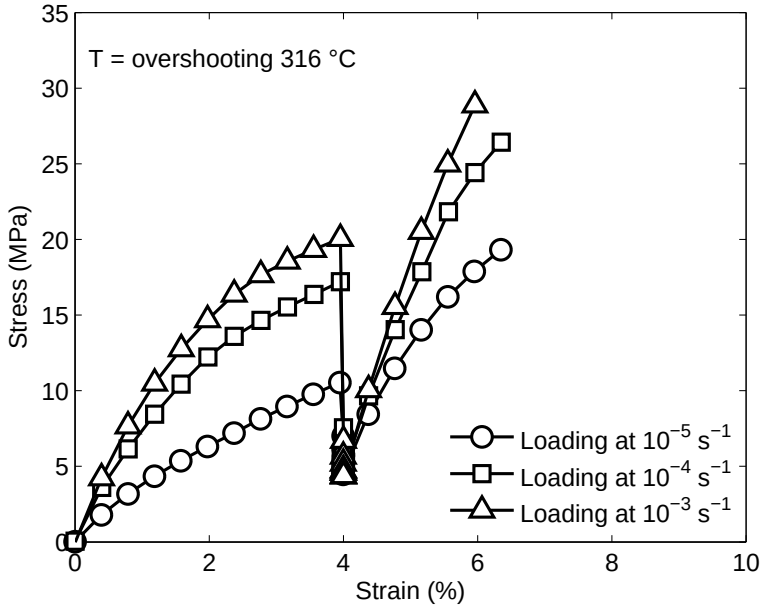

Figure 9.3: Overshooting the Test Temperature of 316 °C. The results of the Monotonic Loading with Single Period of Relaxation are exhibited.

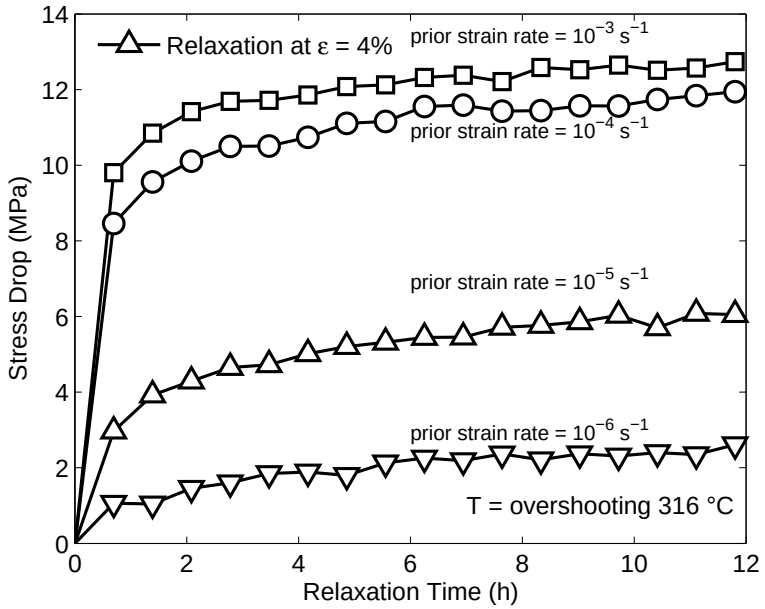

Figure 9.4: Overshooting the Test Temperature of 316 °C. Stress Drop vs Relaxation Time is exhibited.

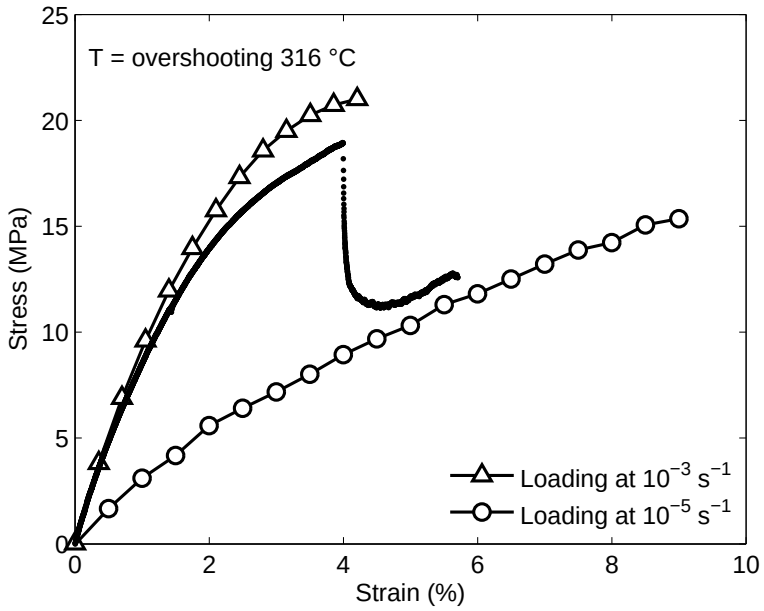

Figure 9.5: Overshooting the Test Temperature of 316 °C. The result of the Strain Rate Jump Test is exhibited.

It has been demonstrated in this chapter that overshooting the temperature 316 °C does influence the mechanical behavior of the PMR-15. The key features of material which were reasonably expected and similar to the behaviors seen in the tests conducted at 316 °C include:

- positive, nonlinear strain rate sensitivity in monotonic loading,
- no strain rate history effect in the strain rate jump test,
- dependence of relaxation behavior on the prior strain rate magnitude.

The unique features observed when overshooting 316 °C were:

- the material shows a reduction in strength in both Monotonic Loading and Loading and Unloading Tests. Likewise, a reduction in strength is profoundly exhibited in Monotonic Loading with Single Period of Relaxation,
- once the loading is resumed in Monotonic Loading with Single Period of Relaxation Tests, stress strain curves overshoots the initial flow stress level. The overshooting is more pronounced when compared to those at 316 °C.

- The decrease in stress drops during relaxation is clearly influenced by the test temperature. A larger decrease in stress is observed in relaxation following loading with all the strain rates at 316 °C.

X. Conclusions and Recommendations

10.1 Concluding Remarks

The inelastic deformation behavior of unaged PMR-15 neat resin was investigated at 316 °C. Experimental results revealed the rate dependence of the inelastic deformation. The unaged PMR-15 neat resin exhibits positive nonlinear strain rate sensitivity during monotonic loading and unloading. In monotonic loading at higher strain rates material exhibits inability to establish inelastic flow fully and early failures are observed. The flow stress level increases with the increasing prior strain rate. There is no strain rate history effect in the strain rate jump test. The recovery of strain at zero stress is profoundly affected by prior strain rate. The recovery rate increases with prior strain rate. Creep behavior is also strongly influenced by the prior strain rate. Creep rate at the same stress level increases with prior strain rate. In the same manner, relaxation behavior is influenced by prior loading rate. It seems that the stress values at the end of the relaxation periods comes to rest which forms of a stress-strain diagram and is positioned below the stress-strain curves obtained for the slowest prior loading rate. This behavior suggests the existence of an equilibrium stress curve with the shape similar to that of the stress-strain curve obtained at 10^{-6} s^{-1}. And also once the monotonic loading is resumed after the relaxation inelastic flow is never reached before failure. These experimental investigations revealed several qualitative features of the inelastic deformation behavior of the PMR-15 neat resin that strongly suggest the usefulness of the overstress constitutive model.

The Viscoplasticity Based on Overstress for Polymers (VBOP) was chosen for constitutive modeling. A limited set of experiments needed to characterize the VBOP parameters was identified in this effort. The model characterization process that was proposed by McClung [9] for PMR-15 at 288 °C was used for the case of PMR-15 at 316 °C. The characterization method relies on experimental data and eliminates the uncertain and time-consuming "guess-and-check" approach to determining model parameters. The model capabilities and the model characterization procedure were evaluated by comparing the model predictions with the experimental results obtained

in tests that were not used for model characterization. The simulations of the deformation behavior of the unaged material under strain-controlled and stress-controlled tests histories were in good agreement with the experimental data. The model was unable to accurately predict the unloading stress-strain behavior of the PMR-15 polymer at 316 °C.

The effects of prior aging in argon at 316 °C on the time dependent deformation behavior of the PMR-15 at 316 °C were examined by means of the monotonic tensile tests conducted at constant strain rates. The experimental results clearly demonstrate that prior aging in argon influences the rate-dependent behavior of the PMR-15 polymer. The specimens, which are subjected to prior aging in argon for more than 50 h, exhibit only quasi-linear behavior until failure. Furthermore, transition to inelastic flow is no longer observed. The specimens aged over 50 h show an inability to strain past the region of quasi-elastic behavior at strain rates of 10^{-6}, 10^{-5}, 10^{-4}, and 10^{-3} s^{-1}. In addition to the reduced capacity for inelastic straining, the material shows a reduction in strength for aging durations above 100 h. And there exists early failures.

10.2 Comparison with the Previous Work

There were several features of the unaged PMR-15 behavior demonstrated in the current research which were reasonably expected and similar to the behaviors seen in previous effort include:

- positive, nonlinear strain rate sensitivity in monotonic loading,
- dependence of recovery behavior on the prior strain rate magnitude,
- dependence of creep rate on the prior strain (loading) rate,
- no strain rate history effect in the strain rate jump test,
- dependence of relaxation behavior on the prior strain rate magnitude.

The unique features of the unaged PMR-15 at 316 °C were:

- In monotonic loading at higher strain rates material exhibits inability to establish inelastic flow fully and early failures are observed,
- Likewise, once the monotonic loading is resumed after the relaxation inelastic flow is never reached before failure.

The similar or expected effects of the prior aging included the reduced capacity for inelastic straining and the reduction in strength. But the effects of the prior aging that were exhibited in the previous efforts were not observed in this study. Instead the following observations were stated: The specimens, which are subjected to prior aging in argon for more than 50 h, exhibit only quasi-linear behavior until failure. And transition to inelastic flow is no longer observed.

10.3 Recommendations

The most challenging part of this effort was to conduct the experiments at the temperature of 316 °C since this temperature was so close to T_g. In the previous effort [20] it was reported that the unaged PMR-15 neat resin found to have a T_g of 331 °C. Therefore it was so easy to overshoot the temperature. Furthermore, the temperature of the specimen gauge section was controlled by an MTS resistance-heated furnace, with an MTS temperature controller. The problem with the MTS temperature controller was to control only the left furnace temperature and to accept the temperature on the right furnace whatever it reads. And the difference between two readings can reach up to 7 °C. With the aging thermocouples this discrepancy even gets worse going beyond the 10 °C. Considering the closeness of the test temperature and the T_g, this amount is huge. And the room temperature that was observed during the tests varied a lot. It was 23 °C in the daytime and 30 °C in the night. Considering the duration of the tests, this temperature difference in the lab has an effect on the test results. Future efforts may have more temperature sensitive conditions.

As it was stated in the previous effort once more, future modeling efforts of the behavior of the PMR-15 neat resin may involve developments of the VBOP for-

mulation to address the unloading stress-strain behavior. Furthermore, this effort investigates the PMR-15 neat resin which is used as a matrix material in high temperature PMC's. Similar studies may be processed for the PMR-15 based composites to investigate the effects of prior aging and the interactions between the neat resin matrix and the reinforcement material. In addition, modeling efforts may be extended to predict the rate dependent behavior of polymer based composite materials which play a critical role in critical load-bearing structures.

Bibliography

1. P. J. Waterman, "The life of composite materials," Design Engineering Magazine. Online, November 6, 2008, http://66.195.41.10/Articles/Feature/The-Life-of-Composite-Materials-200704101800.html.

2. C. L. Brinson *et al.*, *Going to Extremes Meeting the Emerging Demand for Polymer Matrix Composites.* Washington DC, the National Academies Press, 2005.

3. J. A. S. Green *et al.*, *New Materials for Next Generation Commercial Transports.* Washington DC, the National Academies Press, 1996.

4. C. M. Falcone, "Some aspects of the mechanical response of PMR-15 neat resin at 288 °C: Experiment and modeling," Master's Thesis, Department of Aeronautics and Astronautics, Air Force Institute of Technology, Wright Patterson Air Force Base, Ohio, 2006.

5. W. Xie, W. P. Pan and K. C. Chuang, "Thermal degradation study of polymerization of monomeric reactants (PMR) polyimides," *Journal of Thermal Analysis and Calorimetry*, vol. 74, pp. 477–485, 2001.

6. A. J. W. McClung and M. B.Ruggles-Wrenn, "The rate (time) - dependent mechanical behavior of the PMR-15 thermoset polymer at elevated temperature," *Polymer Testing*, vol. 27, pp. 908–914, 2008.

7. NASA, "DMBZ polyimides provide an alternative to PMR-15 for high-temperature applications," Online, Tech. Rep., July 2007, Http://www.grc.nasa.gov/WWW/RT/RT1995/5000/5150c.htm.

8. C. M. Falcone and M. B. Ruggles-Wrenn, "Rate dependence and short-term creep behavior of a thermoset polymer at elevated temperature," *Journal of Pressure Vessel Technology, Trans ASME*, 2009.

9. A. J. W. McClung, "Extension of viscoplasticity based on overstress to capture the effects of prior aging on the time dependent deformation of a high-temperature polymer: Experiments and modeling," Ph.D Thesis, Department of Aeronautics and Astronautics, Air Force Institute of Technology, Wright Patterson Air Force Base, Ohio, 2008.

10. C. M. Westberry, "Rate dependence and short-term creep behavior of PMR-15 neat resin at 23 and 288 °C," Master's Thesis, Department of Aeronautics and Astronautics, Air Force Institute of Technology, Wright Patterson Air Force Base, Ohio, 2005.

11. M. B. Ruggles-Wrenn and J. G. Balaconis, "Some aspects of the mechanical response of BMI 5250-4 neat resin at 191 °C: Experiment and modeling," *Journal of Applied Polymer Science*, vol. 107, pp. 1378–1386, 2008.

12. C. M. Bordonaro, "Rate dependent mechanical behavior of high strength plastics: Experiment and modeling," Ph.D. thesis, Department of Mechanical Engineering, Aeronautical Engineering and Mechanics, Rensselaer Polytechnic Institute, Troy, NY, 1995.

13. E. Krempl and C. M. Bordonaro, "A state variable model for high strength polymers," *Polymer Engineering and Science*, vol. 35, no. 4, pp. 310–316, 1995.

14. F. Khan, "The deformation behavior of solid polymers and modeling with the viscoplasticity theory based on overstress," Ph.D. thesis, Department of Mechanical Engineering, Aeronautical Engineering and Mechanics, Rensselaer Polytechnic Institute, Troy, NY, 2002.

15. K. Ho, "Application of the viscoplasticity theory based on overstress to the modeling of dynamic strain aging of metals and to the modeling of the solid polymers, specifically to nylon 66," Ph.D. thesis, Department of Mechanical Engineering, Aeronautical Engineering and Mechanics, Rensselaer Polytechnic Institute, Troy, NY, 1998.

16. E. Krempl and K. Ho, "An overstress model for solid polymer deformation behavior applied to nylon 66," in *Time Dependent and Nonlinear Effects in Polymers and Composites*, ser. Proceedings of the ASTM Symposium, Atlanta, GA; UNITED STATES; 4-5 May 1998, R. A. Schapery and C. T. Sun, Eds., vol. 1357 of ASTM STP. West Conshohocken, PA: American Society for Testing and Materials, 2000, pp. 118–137.

17. F. Khan and E. Krempl, "Pre-necking and post-necking relaxation and creep behavior of polycarbonate: A phenomenological study," *Polymer Engineering and Science*, vol. 44, pp. 1783–1791, 2004.

18. F. Khan and E. Krempl, "Amorphous and semicrystalline solid polymers: Experimental and modeling studies of their inelastic deformation behaviors," *J Eng Mater Technol, Trans ASME*, vol. 128, 2006.

19. C. M. Bordonaro and E. Krempl, "Effects of strain rate on the deformation and relaxation behavior of 6/6 nylon at room temperature," *Polymer Engineering and Science*, vol. 32, no. 16, pp. 1066–1072, 1992.

20. J. L. Broeckert, "Effects of prior aging at 288 °C in air and in argon environments on creep response of PMR-15 neat resin," Master's Thesis, Department of Aeronautics and Astronautics, Air Force Institute of Technology, Wright Patterson Air Force Base, Ohio, 2007.

21. M. B. Ruggles-Wrenn and J. L. Broeckert, "Effects of prior aging at 288 °C in air and in argon environments on creep response of PMR-15 neat resin," *Journal of Applied Polymer Science*, 2008.

22. K. J. Bowles, D. S. Papadopoulos, L. L. Ingrham, L. S. McCorkle and O. V. Klah, "Longtime durability of PMR-15 matrix polymer at 204, 260, 288, and 316 °C," TM 210602, NASA/Glenn Research Center, 2001.

23. G. P. Tandon, K. V. Pochiraju and G. A. Schoeppner, "Modeling of oxidative development in PMR-15 neat resin," *Polymer Degradation and Stability*, vol. 91, no. 8, pp. 1861–1869, August 2006.

24. G. A. Schoeppner, G. P. Tandon and E. R. Ripberger, "Anisotropic oxidation and weight loss in PMR-15 composites," *Applied Science and Manufacturing*, vol. 38, no. 3, pp. 890–904, March 2007.

25. C. G. Ladrido, "Effect of prior aging on fatigue response of IM7/BMI 5250-4 composite at 191 °C," Master's Thesis, Department of Aeronautics and Astronautics, Air Force Institute of Technology, Wright Patterson Air Force Base, Ohio, 2007.

26. R. Hall, G. Schoeppner, K. Pochiraju, G. Tandon, E. Iarve and E. Mollenhauer, "Progress toward thermodynamic environmental durability modeling of high temperature polymer matrix composites," in *Proceedings of the 5th International Conference on Mechanics of Time Dependent Materials*, October 2005.

27. C. Marias and G. Villoutrex, "Analyses and modeling of the creep behavior of the thermostable PMR-15 polymide," *Journal of Applied Polymer Science*, vol. 69, pp. 1983–1991, 1998.

28. I. M. Daniel and O. Ishai, *Engineering Mechanics of Composite Materials*. Oxford University Press, 1994.

29. E. Riande *et al.*, *Polymer Viscoelasticity: Stress and Strain in Practice*. Marcel Dekker, Inc, 2000.

30. P. A. Lovell and R. J. Young, *Introduction to Polymers*, 2nd ed. Chapman and Hall Publishing, 1991.

31. J. R. White, "Polymer ageing: physics, chemistry or engineering? Time to reflect," *Science Direct*, pp. 1396–1408, 2006.

32. E. Krempl, "Cyclic creep: An interpretive literature survey," *Weld. Res. Counc. Bull.*, no. 195, pp. 63–123, June 1974.

33. E. Krempl, "The role of aging in the modeling of elevated temperature deformation," in *Creep and Fracture of Engineering Materials and Structures*, ser. Proceedings of the International Conference, B. Wilshire and D. R. J. Owen, Eds. University College, Swansea, Wales: Pineridge Press, March 1981, pp. 201–211.

34. E. Krempl, "Viscoplasticity based on total strain. the modeling of creep with special considerations of initial strain and aging," *J Eng Mater Technol, Trans of the ASME*, vol. 101, no. 4, pp. 380–386, October 1979.

35. M. B. Ruggles and E. Krempl, "Rate-sensitivity and short term relaxation behavior of AISI type 304 stainless steel at room temperature and at 650 °C; influence of prior aging," *Journal of Pressure Vessel Technology, Trans ASME*, vol. 113, no. 3, pp. 385–391, August 1991.

36. E. Krempl, *Unified Constitutive Laws of Plastic Deformation.* San Diego: Academic Press, 1996.

37. E. Krempl, "From the standard linear solid to the viscoplasticity theory based on overstress," in *Computational Mechanics '95 Theory and Applications*, ser. Proceedings of the International Conference on Computational Engineering Science, G. Y. S. N. Atluri and T. A. Cruse, Eds., vol. 2. Hawaii: Springer, July-August 1995, pp. 1679–1684.

38. E. Krempl, J. J. McMahon and D. Yao, "Viscoplasticity based on overstress with a differential growth law for the equilibrium stress," ser. Nonlinear Consti-tutive Relations for High Temperature Application-1984, Symposium Proceedings, vol. 2369, NASA, Lewis Research Center. NASA Conference Publication, June 1985, pp. 35–50.

39. J. Scheirs, *Compositional and Failure Analysis of Polymers.* Wiley and Sons LTD., 2000.

40. M. B. Ruggles, S. Cheng and E. Krempl, "The rate dependent mechanical behavior of modified 9 wt. Cr-1 wt. Mo steel at 538 °C," *Materials Science and Engineering*, vol. A186, no. 1-2, pp. 15–21, 1994.

REPORT DOCUMENTATION PAGE

Form Approved
OMB No. 0704–0188

1. REPORT DATE *(DD–MM–YYYY)*	2. REPORT TYPE	3. DATES COVERED *(From — To)*
26–03–2009	Master's Thesis	Sept 2007 — Mar 2009

4. TITLE AND SUBTITLE

Effects of Prior Aging at 316 °C in Argon on Inelastic Deformation Behavior of PMR-15 Polymer at 316 °C : Experiment and Modeling

5a. CONTRACT NUMBER

5b. GRANT NUMBER

5c. PROGRAM ELEMENT NUMBER

6. AUTHOR(S)

Ozgur Ozmen, 1st Lt, USAF

5d. PROJECT NUMBER

5e. TASK NUMBER

5f. WORK UNIT NUMBER

7. PERFORMING ORGANIZATION NAME(S) AND ADDRESS(ES)

Air Force Institute of Technology
Graduate School of Engineering and Management (AFIT/EN)
2950 Hobson Way
WPAFB OH 45433-7765

8. PERFORMING ORGANIZATION REPORT NUMBER

AFIT/GSS/ENY/09-M06

9. SPONSORING / MONITORING AGENCY NAME(S) AND ADDRESS(ES)

Dr. Charles Y.C. Lee
Air Force Office of Scientific Research (AFSOR)
875 N Randolph St. Suite325 Rm. 3112
Arlington VA 22203

10. SPONSOR/MONITOR'S ACRONYM(S)

AFSOR

11. SPONSOR/MONITOR'S REPORT NUMBER(S)

12. DISTRIBUTION / AVAILABILITY STATEMENT

Approval for public release; distribution is unlimited.

13. SUPPLEMENTARY NOTES

14. ABSTRACT

The inelastic deformation behavior of PMR-15 neat resin, a high-temperature polymer, was investigated at 316 °C. The experimental program was designed to explore the influence of strain rate on tensile loading, unloading, and strain recovery behaviors. In addition, the effect of the prior strain rate on the relaxation response of the material, as well as on the creep behavior following strain controlled loading were examined. The material exhibits positive, nonlinear strain rate sensitivity in monotonic loading and unloading. Early failures occur in the inelastic regime. The recovery of strain at zero stress and creep response are strongly affected by prior strain rate. The prior strain rate also has a profound influence on relaxation behavior. The experimental data were modeled with the Viscoplasticity Based on Overstress (VBO) theory. Additionally the effects of prior aging at 316 °C in argon on the time (rate)-dependent behavior of the PMR-15 polymer were evaluated in a series of strain controlled experiments. Based on experimental results, it was stated that the specimens, which are subjected to prior aging in argon for more than 50 h, exhibit only quasi-linear behavior until failure.

15. SUBJECT TERMS

polymer, PMR-15, creep, recovery, relaxation, prior strain rate, nonlinear viscoplastic theory, aging

16. SECURITY CLASSIFICATION OF:			17. LIMITATION OF ABSTRACT	18. NUMBER OF PAGES	19a. NAME OF RESPONSIBLE PERSON
a. REPORT	b. ABSTRACT	c. THIS PAGE			Marina B. Ruggles-Wrenn, PhD
U	U	U	UU	95	19b. TELEPHONE NUMBER *(include area code)* (937)255-3636x4641